Understanding the interannual variability of pCO_2 in the sea-ice impacted Southern Ocean

By Bongiwe Jojo
(JJXBON001)

Department of Oceanography
University of Cape Town
Rondebosch, Cape Town
South Africa

Supervisor (s): Prof V Marcello

Co-supervisors: Dr S Nicholson

Dr M Du Plessis

30 November 2023

Dissertation submitted in partial fulfilment of the requirements for the degree of Master of Science (by coursework and dissertation) in Applied Ocean Sciences, through the Marine and Antarctic Research Centre for Innovation and Sustainability (MARiS), in the Department of Oceanography, at the University of Cape Town

Plagiarism Declaration

I, Bongiwe Nokuthula Patience Jojo, hereby:

1. grant the University of Cape Town a free license to reproduce the above thesis in whole or in part, for the purpose of research.
2. declare that:

   (a) this dissertation is my unaided work, both in concept and execution and apart from the normal guidance from my supervisor, I have received no assistance except as acknowledged.

   (b) neither the substance nor any part of the above dissertation has been submitted in the past or is being or is to be submitted for a degree at this University or at any other university.

Signed by candidate

Bongiwe Nokuthula Patience Jojo

Student's Full Name

Department of Oceanography
University of Cape Town

Thursday 16 November 2023

Abstract

Sea-ice is permeable and plays an active role in the marine carbon cycle via biological and physio-chemical processes. The carbon cycle in seasonally sea-ice-covered waters needs to be better understood due to a lack of observational data and the system's complexity. To characterize the interannual variability of oceanic pCO_2 in the sea-ice-impacted Southern Ocean and identify their potential primary drivers, this thesis combines in situ observations with remotely sensed data and reanalysis models during the austral summer months. The region of focus is divided into three sections: the Southern Ocean, three ocean basins, and the Goodhope line transect. Averaged over the Southern Ocean, the range of year-to-year variability of pCO_2 between 2000 to 2018 was between 290 atm (2004) and 355 atm (2003). It is also noted that the interannual variability in pCO_2 does not correspond to that of the Southern Annular Mode (SAM) index; however, there are some indications that the SAM may be an essential driver on longer time scales. Noticeably, the year 2016 stands out as one of the warmest and has the smallest Antarctic sea-ice extent (SIE) recorded since 1979 in the Southern Hemisphere. This SIE reduction has been attributed to positive sea surface temperature anomalies, the zonal wave pattern 3, and a SAM negative phase. pCO_2 decreased in response to this ice loss event highlighting its sensitivity to rapid changes in sea ice. Overall, salinity obtains the highest correlation to the annually averaged pCO_2 in the Southern Ocean and various basins. Along the Goodhope Line, variability of pCO_2 indicated a higher magnitude and interannual variability of pCO_2 during early summer than late summer. Non-thermal drivers primarily explain the variability of pCO_2. These results suggest that the leading causes of the interannual variability of pCO_2 in the sea ice-impacted Southern Ocean are those associated with non-thermal drivers of pCO_2.

Acknowledgments

I would like to express my utmost gratitude and appreciation to Dr Sarah Nicholson and Dr Marcel du Plessis, for their unwavering support, patience, dedication, and faith in me. Their continuous encouragement gave me all the strength and eagerness throughout the entire dissertation process. Their fountain of knowledge in oceanography and research has been evident in every aspect of this dissertation (including but not limited to coding and unique writing skills). Their dedication and work ethic in the science field are some of the values I aspire to emulate throughout my career.

I'm sincerely grateful to Prof M Vichi, for his continuous support, and all the academic/administration advice he has provided me with throughout this journey. As a thoughtful instructor, he played a role in introducing some of the fundamentals of oceanography.

I would also like to express my gratitude to the Council for Scientific and Industrial Research for the financial support provided.

I'm forever thankful for the unconditional love and support throughout the entire dissertation process and every day.

Table of Content

Acronyms

CO_2	- Carbon dioxide
pCO_2	– Partial pressure of carbon dioxide
SO	- Southern Ocean
CDW	- Circumpolar Deep Water
SAMW	- Subantarctic Mode Water
AAIW	- Antarctic Intermediate Water
MOC	- Meridional Overturning Circulation
DIC	- Dissolved inorganic carbon
SOCAT	- Surface Ocean CO_2 Atlas
TA	- Total Alkalinity
SAM	- Southern Annular Mode
SST	- Sea surface temperature
DJF	- December, February January
SIZ	- Seasonal ice zone
SSS	- Sea surface salinity

Chapter 1 **Introduction**

1.1 Background

The Southern Ocean plays an important role in the exchange of carbon dioxide between the ocean and the atmosphere (Friedlingstein et al., 2022), and changes in the Southern Ocean therefore have important impacts on the global carbon cycle and climate (Fransson et al., 2011a; Rintoul, 2018, Friedlingstein et al., 2022). With the advent of improved observational capabilities and new empirical analysis techniques (e.g., machine learning), annual to multidecadal changes in CO_2 can now be better resolved (e.g., both spatially and temporally), these data showed a global weakening in CO_2 uptake, followed by a resurgence in global CO_2 uptake, mainly driven by changes in the Southern Ocean associated with responses to interannual to interdecadal wind fluctuations (D. C. E. Bakker et al., 2016; Gruber et al., 2018; Landschützer et al., 2013).

Previous studies conducted by Gregor et al., 2019, and Hague & Vichi, 2018 amongst others have indicated that one of the least studied and least understood areas of the Southern Ocean is the Antarctic Sea Ice Zone (SIZ), where empirical estimates of annual to decadal CO_2 fluxes continue to have large errors between model ensembles. This is due to the lack of observations and understanding of the variability of CO_2 in the Antarctic SIZ and the processes that control air-ocean interactions such as winds, sea ice conditions, temperature, and biological productivity (Fransson et al., 2011). Abernathy et al., 2016, have shown that seasonal growth and retreat of sea ice have been shown to influence upper limb overturning circulation with associated freshwater fluxes altering surface water. Therefore, annual to multidecadal changes in sea ice concentration can have remote and long-term effects on Southern Ocean circulation, which in turn can influence the global carbon cycle. However, few studies have investigated the interannual variability of CO_2 and the associated local atmospheric-sea-ice CO_2 processes that occur in the SIZ and how such processes influence regional CO_2 variability. This study investigates the interannual variability of pCO_2 and the

potential primary drivers of pCO_2 variability over the summer period. This is towards an improved understanding of the importance of the sea-ice-impacted Southern Ocean and its contributions to the variations of seasonal pCO_2 and CO_2 flux for the Southern Ocean.

1.2 Problem statement

How does the seasonal ice impact the interannual variability of pCO_2 and what are the potential drivers of the interannual variation of pCO_2 during summer?

1.3 Project aim & objectives

The study uses a multidisciplinary approach, combining ship-based in situ observations, remote sensing, and reanalysis data to understand interannual variations in pCO_2. This study uses the partial pressure of CO_2 (pCO_2) as the primary measure to diagnose pCO_2 fluctuations. pCO_2 defines the gradient between atmospheric pCO_2 and ocean pCO_2 and is an important parameter underlying CO_2 fluxes (e.g., Wanninkhof et al., 2009). To obtain pCO_2 measurements, we use the already available pCO_2 dataset from the Surface Ocean pCO_2 Atlas (SOCAT). Due to the limited number of observations conducted in Antarctica during the winter, the SOCAT database is seasonally biased towards summer. For this reason, this project will focus on the interannual variations in pCO_2 observed in summer. More specifically, the project aims to:

1. Characterize the interannual variability of pCO_2 in summer in the Antarctic Seasonal Ice Zone

2. To determine the interannual variation in pCO_2 averaged across the SIZ over 18 years and to dynamically characterize regional differences in the interannual variation by dividing the SIZ into different ocean basins and separating and contrasting regions.

3. To interrogate the different drivers of summer pCO2 variability in the Seasonal Ice Zone:

- To perform a regression analysis on the annual time series of pCO_2 (dependent variable) with the independent variables' monthly average primary drivers.
- To investigate the relationship between the interannual variability of pCO_2 and interannual variability of primary drivers (wind stress, sea-ice concentration, salinity, sea surface temperature, and SAM).

1.4 Limitations

This study focuses on the characterization of the interannual variability of pCO_2 in summer over 18 years in the seasonal ice zone and investigates the relationship between the interannual variability in ocean pCO_2 and the interannual viability of primary drivers.

The limitations of, and assumptions applied, in this study are discussed in detail under chapter 5. Broadly, they include:

- Aliasing of the variability due to the spatial coverage and temporal coverage of the observations
- Difficulties in obtaining driver data in the Seasonal Ice Zone. As well as general poor coverage of pCO_2 and the primary drivers' observations used by the study.
- The usage of the SAM index, rather than pressure fields.

Chapter 2 **Introduction**

The Southern Ocean (SO), the circumpolar ocean south of 30° S (Rintoul, 2018), plays a crucial role in mediating global climate through its disproportionate role in absorbing excess heat and carbon dioxide (CO_2) from the atmosphere (Khatiwala et al., 2013; Mikaloff Fletcher et al., 2006; Rintoul, 2018; Sabine et al., 2004). This is evidenced in prognostic coupled climate-carbon models and empirically derived estimates (machine learning reconstructions) based on observations. It is estimated that the SO contributes to approximately 75% of anthropogenic heat uptake and 40% of anthropogenic CO_2 uptake by the global ocean (Friedlingstein et al., 2022; Frölicher & Paynter, 2015). However, there remain substantial uncertainties within both approaches (prognostic and empirical modeling), primarily due to mis- or under-representation of crucial processes and spatiotemporal aliasing (Hewitt et al., 2022; Precious Mongwe et al., 2018).

The unique characteristics of the circulation of the Southern Ocean enable these sinks of heat and CO_2 and make it a central component of the earth's climate. The Southern Ocean flows zonally around Antarctica without being bounded by land masses, connecting all major ocean basins. Here, strong westerly winds drive Ekman divergence of surface waters, resulting in a large-scale upwelling of deep old carbon-rich Circumpolar Deep Waters (CDW) to the surface ocean around the subpolar latitudes. CDW that reaches the surface is exposed to air-sea interactions while being transported northwards, transforming into lighter Subantarctic Mode Water (SAMW) and Antarctic Intermediate Water (AAIW); these water masses form the upper branch of the Meridional Overturning Circulation (MOC). Air-sea interactions are an integral part of the global thermohaline circulation (Ayers & Strutton, 2013; Sloyan & Rintoul, 2001; Speich et al., 2007) in which the SO sits as a central component. This continuous surfacing cycle and subsequent northward displacement of nutrient-rich and cold CDW waters allow the SO to continue absorbing heat and supplying nutrients to the SO, fuelling primary production.

Importantly, this large-scale circulation creates the potential for exchanges of CO_2 between the atmosphere, ocean, and sea ice across the SO. South of the polar front, the large-scale upwelling of CDW CO_2-rich waters close to the surface results in a net weak outgassing flux (positive flux) of CO_2. In contrast, north of it, as the water absorbs heat (decreasing solubility) and fuels primary production (decreasing DIC), a large net sink of CO_2 (negative flux) is present (D. C. E. Bakker et al., 2008; Brown et al., 2015; Ogundare et al., 2021). The gradient of the partial pressure of CO_2 (pCO_2) between the ocean and atmosphere determines the direction of CO_2 flux (Williams et al., 2018). pCO_2 in the ocean is typically far more variable than pCO_2 in the atmosphere, which is mainly mixed; thus, the spatial and temporal variability of pCO_2 at the ocean surface is a dominant control of the gradient, and therefore the carbon flux patterns between the air and the ocean. Therefore, to gain more knowledge about SO carbon fluxes, we need to observe and understand oceanic pCO_2 and the significant factors influencing its variability (Shetye et al., 2015). While substantial progress has been made, particularly through coordinated initiatives such as Surface Ocean CO_2 Atlas (SOCAT), there remain critical regional blind spots in observations and knowledge, such as the sea ice zone and critical temporal modes of variability such as seasonal and intra-seasonal variations of pCO_2 (Monteiro et al., 2015).

In particular, the seasonal cycle is a crucial mode of variability that links longer climate forcing to short-term responses in primary production, diversity, and carbon export in SO (Monteiro et al., 2011; Shetye et al., 2015; Thomalla et al., 2011). Variability in surface ocean pCO_2 content can be separated into thermal and biogeochemical-physical/non-thermal drivers (Keppler & Landschützer, 2019). These drivers influence the seasonal cycle of CO_2 fluxes and include, for example, primary production in summer and mixing in winter (Angeles Gallego et al., 2018; Fay & McKinley, 2017; Takahashi et al., 2002). Variations in the non-thermal component of pCO_2 include fluctuations in alkalinity and DIC, which are influenced by biological activity (primary production) and physical transport (advection and mixing). Seasonal variations in DIC are generally larger (e.g., DIC: Alkalinity ~ 2:1) than alkalinity in the Southern Ocean (Fig. 3, Williams et al., (2018); thus, the DIC seasonal cycle strongly influences the non-thermal component's seasonality (Fay & McKinley, 2017; Freeman et al., 2019; Jiang et al., 2014). Temperature changes explain the thermal component. As temperature rises, the solubility of

the surface water decreases, resulting in a decrease in oceanic pCO_2, while the opposite is true for decreasing temperatures.

In the open-ocean SO, these seasonal drivers are embedded and interact with the MOC's large-scale distributions of heat and CO_2. High temperatures and increased precipitation provide fresh water to the sea, lowering salinity. Low salinity salt water includes low carbonates and other ions, resulting in a large drop in DIC. As seawater alkalinity rises, CO_2 is transferred to DIC species like HCO^{3-} and CO_3^{2-}, lowering the partial pressure of CO_2 (pCO_2). At the ocean surface, this process increases CO_2 flux between the atmosphere and the ocean, leading to net CO_2 uptake. During autumn-winter, deep convective-driven mixing drives entrainment and increased supplies of subsurface CDW waters with high DIC concentrations to the surface, resulting in higher oceanic pCO_2 and potentially outgassing (Lenton et al., 2013; Metzl et al., 2006; Precious Mongwe et al., 2018; Prend et al., 2022; Sarmiento et al., 2004). There are strong zonal variations in the magnitude of this winter outgassing (south of the Polar Frontal Zone, refer to Fig. 1 in Prend et al. 2022), which is strongest in the southern half of the SO due to shoaling CDW to the base of the mixed-layer. These winter-driven changes in DIC (non-thermal) dominate the pCO_2 seasonal cycle despite colder SST and associated changes to the solubility of CO_2 in the surface ocean in wintertime (thermal component). In spring, light availability allows for an increase in primary production, which consumes DIC at the surface and increases the ocean's ability to absorb atmospheric CO_2 (Gregor et al., 2017; Gruber et al., 2009; Le Quéré et al., 2009; Pasquer et al., 2015). The increase in sea surface temperature (SST) in late spring and summer (October, November, and December) reduces the CO_2 solubility at the surface, which may partially counteract the strong biological uptake and reduce CO_2 flux from the atmosphere (Nicholson et al., 2022; Takahashi et al., 2002; Williams et al., 2018). There appears to be a weaker, secondary late summer increase in pCO_2 in February and March, likely due to warm SST and decreasing solubility (Doddridge & Marshall, 2017; Matear et al., 2000; Williams et al., 2018). This phenomenon was observed in 2008-2012, indicating the importance of the solubility pump (Landschützer et al., 2018). The total seasonal cycle of pCO2 equates to the net balance of these opposing processes (warming and cooling processes) (Gruber et al., 2018). Until recently, there has

been a minimal investigation into the seasonal-interannual variations of ocean pCO_2 in the sea-ice-influenced Southern Ocean (e.g., impacted by sea-ice melt/formation). This large region contributes to significant uncertainty in the overall magnitude of SO pCO_2 and, subsequently, the global carbon flux (Fay & McKinley, 2013; Gregor et al., 2019; Majkut et al., 2014).

The sea-ice zone (SIZ) surrounding Antarctica is the marine area extending from the permanent ice zone to the boundary where the winter sea-ice extent is greatest. The SIZ, which has an extent of 18 million km^2, experiences maximum annual sea-ice growth of 18.5×10^6 km^2 and minimum annual sea-ice melt of 3.1×10^6 km^2. This sea-ice concentration variation modifies surface waters, increasing freshwater flux (during melt), and directly affects large-scale upwelling carbon-rich CDW waters due to circulation and stratification patterns, turbidity, and nutrient pathways (Abernathey et al., 2016; Pitcher et al., 2010). The SIZ plays a critical role in the air-sea pCO_2 flux, with sea-ice growth and melt controlling the extent of pCO_2 exchange between the ocean surface and the atmosphere through stratification (Geilfus et al., 2016; Grimm et al., 2016). In winter, water crystallizes at the sea surface and forms ice by precipitating brine from the crystal lattice of ice (Eayrs et al., 2019; Fransson et al., 2013; Geilfus et al., 2016). This process is the leading cause of deep-water formation and contributes to water formation with high CO_2 content (Nomura et al., 2006; Rysgaard et al., 2007). In addition, sea-ice growth in winter can inhibit the release of CO_2 from the sea surface to the atmosphere (Shadwick et al., 2021), leading to the accumulation of CO_2 beneath sea-ice, although some studies suggest that CO_2 is released directly from sea-ice (Geilfus et al., 2013; Miller et al., 2011; Nomura et al., 2006). In summer, SST increases, causing sea-ice to melt, leaving a freshwater lens on the sea surface, and causing stratification to increase (Eayrs et al., 2019; I. Giddy et al., 2021). In a study by Nakaoka et al. (2009), the water column's biology and stratification impact oceanic pCO_2 by suppressing the upwelling of suspended particles from bottom waters, improving transparency, and decreasing the amount of pCO_2 in the surface water. This strong sea-ice-induced stratification increases light availability enhancing biological production; it also, however, may reduce shorter-term (sub-

seasonal) vertical fluxes (e.g., storm-driven DIC entrainment events, Nicholson et al. 2022) through the summer as evidenced in Giddy et al. (2021), impacting DIC and associated pCO_2.

In the SO, Landschützer et al. (2016) suggested that the interannual variability of CO_2 is related to the decades-long variability of the Southern Annular Mode (SAM), the dominant mode of atmospheric variability in the Southern Hemisphere (Doddridge & Marshall, 2017; Gregor et al., 2018; Marshall & Speer, 2012). The SAM is characterized by changes in atmospheric mass between 20° S and 90° S (e.g., Thompson & Solomon, 2002; Visbeck & Hall, 2004). The SAM is the leading empirical orthogonal function in several variables: geopotential height, surface temperature, surface pressure, and zonal winds (Thompson & Solomon, 2002). Zonal asymmetry of the SAM is linked with the El Niño – Southern Oscillation and is strongest in winter, particularly over the Pacific sector of the Southern Ocean during a positive phase, thus in accord with the Pacific–Indian winter wind stress dipole (Barnes & Hartmann, 2010; Fogt et al., 2012). According to Sallée et al., (2010), the SAM impacts the winter mixed layer (asymmetry), while Prend et al. (2022) show that the winter mixed layer asymmetry drives the CO_2 outgassing through different winter entrainments. Fogt et al. (2012) noted that the SAM has become more zonally symmetric in summer since the 1980s.

Positive SAM anomalies are associated with a strengthening and poleward shift of midlatitude westerlies over the SO (Thompson & Solomon, 2002). Observational data show a statistically significant trend toward a more positive SAM phase in recent decades (Doddridge & Marshall, 2017). This increase has a seasonal bias; the effect is most influential in the austral summer (DJF). A positive SAM phase correlates with anomalous outgassing of CO_2 between ~ 50 °S and ~ 65 °S in both the Pacific and Indian sectors. In contrast, the opposite is observed for the Atlantic sector, possibly illustrating the impacts of the zonal SAM asymmetry on mixed layer dynamics (Sallée et al., 2010). North of the polar front in the Pacific sector, anomalous outgassing occurs, while south of the polar front in the Atlantic sector, anomalous carbon uptake occurs. The regionally opposed impacts, however, cancel out for the entire SO. The net CO_2 flux on each of the three sectors is 0.0 PgC per year after integrating the total effect of SAM on carbon sequestration from 35° S of SO (Hauck et al., 2013; Keppler & Landschützer,

2019; Lenton & Matear, 2007; Lovenduski et al., 2007). However, the strong zonal asymmetry in the coupling mechanisms between the SAM, mixed layer physics, and outgassing motivates further research in this area, as changes in the coupled mechanisms may lead to future changes in the net flux. Atmospheric inversion and model-based studies have also shown balanced positive and negative correlations between CO_2 flux from the air to the ocean and SAM over the Southern Ocean (Hauck et al., 2013; Lenton & Matear, 2007; Lovenduski et al., 2007). Although some authors show neutral flux from opposing zones, others such as Keppler & Landschützer, 2019, have indicated a slightly positive uptake, albeit based on the model output. These studies showed a slightly positive net integrated uptake of ~0.1 PgC yr^{-1} from 1958 to 2017. It is logical to explore and quantify whether the SAM and thermal and non-thermal drivers play a vital role in the SIZ's interannual and seasonal variability of pCO_2.

The Antarctic SIZ is one of the least studied and, therefore, least understood regions of the global ocean. It is a region where there are not only substantial biases in estimates of interannual to decadal CO_2 fluxes (e.g., Gregor et al., 2019) but also substantial discrepancies between model ensembles of CO_2 flux (e.g., Hague & Vichi, 2018). It still needs to be determined how changes in this region, which includes much of the surface area of the SO, will affect CO_2 variability in the long term. Key to understanding how this region might change is understanding its variability. There needs to be more knowledge of the interannual variability of pCO_2 and potential drivers of pCO_2 variability in summer in the SIZ. This dissertation aims to determine the interannual variability of ocean pCO_2 (spatially and temporally) and the magnitude of this variability across different years and relate this to potential drivers. The interannual variability of ocean pCO_2 in the sea-ice-influenced region of the SO will be examined using an interdisciplinary method integrating observations, remote sensing data, and model analysis. Thermal and non-thermal drivers will be investigated to determine which surface features dominate the interannual changes in pCO_2 during the summer months.

Chapter 3 **Methods**

In this section, I first describe the observational databases that were required to carry out the objectives of this study; then, I discuss the details of the data quality control and data analysis steps. In the remainder of this thesis, I will refer to ocean pCO_2 as simply 'pCO_2'.

3.1 The SOCAT Database

The sea-ice covering the Southern Ocean could be spatially and temporarily sampled more widely and frequently. However, the technical challenge of sampling in sea-ice, the remoteness, and challenging weather conditions, make these crucial observations difficult to achieve. However, over the years, the number of observations made in this region has increased substantially due to the repeat cruise transects, moorings, and autonomous observations (Fig. 1). One of the central observational databases that have become readily available is the Surface Ocean CO_2 Atlas (SOCAT, Bakker et al., 2016). This database merges surface ocean CO_2 data obtained from research ships, commercial ships, moorings, and drifting autonomous surface platforms, providing a collation of data from 1970 to the present (Fig. 1b). The data used for this project is the fugacity of CO_2 (fCO_2) - that is, the pCO_2 equivalent corrected for the non-ideal behavior of the gas -measured in the surface ocean obtained from the Surface Ocean CO_2 Atlas (SOCAT) version 2019. This version consists of 28.2 million in situ surface ocean fCO_2 measurements for the global and coastal seas with an accuracy of < 5 µatm. Furthermore, the SOCAT also provides corresponding surface properties such as salinity and temperature and are used in this study. The measurements are quality-controlled (Bakker et al., 2016) and assembled in the SOCAT and GLODAP synthesis products. Thus, these estimates of fCO_2 are reliable and are used widely by the CO_2 community, particularly for contributing towards the annual global carbon budget (Le Quéré et al., 2009), Intergovernmental Panel on Climate Change assessment, and other high-impact reports that provide international climate regulations.

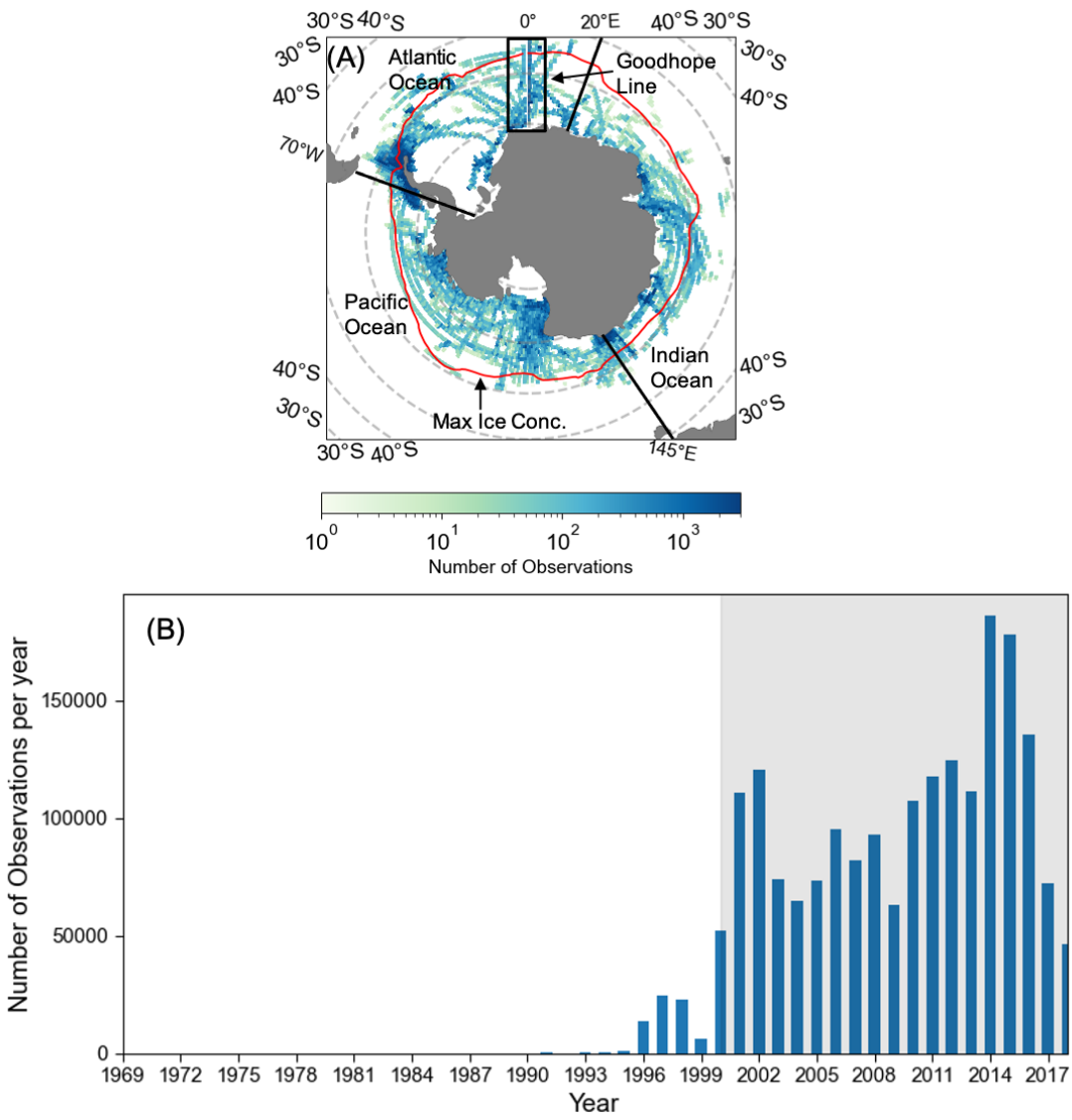

Figure 1: (a) The spatial distribution of pCO_2 with the sea-ice maximum concentration contour (red line) and the Goodhope Line region identified by the black box along the prime meridian. (b) Temporal distribution of pCO_2 observations in the Southern Ocean over 49 years

Fig. 1a shows the spatial distribution of pCO_2 observations in the seasonally covered sea-ice region of the Southern Ocean. Here, repeat cruise lines (ships that follow the same cruise track yearly) are evidenced by regions of higher observational counts (dark blue). However, pCO_2 observations are not evenly spread across the Southern Ocean; instead, the observations are made within specific regions (Fig. 1a). To analyze sectoral variations inside the Southern Ocean, I define the Atlantic sector from 70°W to 20°E, the Indian sector from 20°E to 145°E, and the Pacific sector from 145°E to 70°W (see Fig. 1a). Furthermore, repeat (yearly and seasonal) transects have provided observations in regions of national logistic

voyages to Antarctic bases (e.g., Palmer, SANAE). The analysis also focuses on the Goodhope Line (marked by the black box in Fig. 1a) located between 5 °E - 5 °W, 50 °S - 89°S. This region is investigated to determine the interannual variability of pCO_2 and the possible drivers associated with the variability. This region has gained high traction through different research cruises headed to different regions in the SO (SANAE), leading to an increase in the number of observations made in this region over the years.

3.2 Sea-ice concentration dataset

This study used monthly sea-ice concentration estimates provided by the NCEP-DOE Reanalysis 2 project (NCEP2) (Kanamitsu et al., 2002). NCEP2 is an analysis/forecast system that uses past satellite data from 1979 through the previous year for data assimilation. I used the NCEP2 global T62 Gaussian grid (192x94) data with a temporal coverage of 4-time and monthly values for 1979/01 to 2020/07. As the SOCAT data comprises point observations, the NCEP2 gridded sea-ice concentration product was co-located to the time and location of the SOCAT data. This is done to provide a spatial correlation between the interannual pCO_2 variability and sea-ice concentration across the SIZ over the corresponding 49-year period.

3.3 Wind speed dataset

The wind speed data will be used to determine the influence and the magnitude of the influence of wind on pCO_2. This analysis will explain whether the wind is the primary driver of the variability of pCO_2. The European Centre for Medium Weather Forecasting (ECMWF) provides an hourly, 31 km reanalysis called ERA5, produced using the 4D-Var data assimilation in CY41R2 of ECMWF's Integrated Forecast System (IFS). I use ERA5 as it provides data at an hourly frequency and has a high spatial resolution relative to other products. The variability of the wind will be determined by averaging the data monthly and annually. Further motivation for choosing this wind product is that it has been shown to perform well (i.e., the correlation coefficient of 0.75) compared to in situ wind speed observations carried out close to the sea-ice edge (Swart et al., 2023).

3.4 Data quality and control analysis

The SOCAT dataset-to-data contains the most extensive collection of measurements of the surface ocean pCO_2 and fCO_2. This study was based on the dataset that reported sea surface CO_2 concentration as fCO_2. The computation of fCO_2 requires only temperature and pCO_2, whereas that of pCO_2 in seawater requires temperature, total CO_2 concentration, pH (alkalinity), and salinity (Takahashi et al., 1993). In most cases, fCO_2 values are within a few µatm of pCO_2 (Weiss, RF., 1974). For this reason, fCO_2 was recomputed to the partial pressure of carbon dioxide (pCO_2) and further used for all analyses. fCO_2 was converted to pCO_2 using the SeaFlux python toolbox (https://github.com/lukegre/SeaFlux, (Fay et al., 2021)) following software developed by Pierrot et al. (2009). The wind speed and sea-ice concentration were then spatially and temporally co-located with the SOCAT-derived pCO_2 measurements.

The data analysis involves three analysis steps to achieve the aim of this project, which is to understand the interannual variability of pCO_2 in the SIZ. These steps are detailed below.

Step 1: Quality control and data selection

Fig. 2a, a box whisker plot of pCO_2 for 49 years of all SOCAT observations in the SO, provides the median value of pCO_2, lower and upper quartiles, and outliers. The data was then restricted based on the pCO_2 values between 200 µatm and 500 µatm to remove any anomalous points of pCO_2 measurements in the SIZ that may obscure the mean value (which represents the interannual variability of pCO_2). Also, the spareness of the data in the earlier years was not considered in the analysis. Fig 2b shows a distribution of pCO_2 observations according to two seasons: early/late summer and winter. Based on this distribution, it can be observed that there is a disproportion in the number of observations made in winter and summer. Many observations are made during late and early summer and less in winter. This limitation in the number of observations carried out during the winter months in the Southern Ocean can be attributed to the seasonal (summer) bias in the SOCAT database. For this

reason, the SIZ pCO_2 observations were isolated seasonally only to include summer months, December, January, and February.

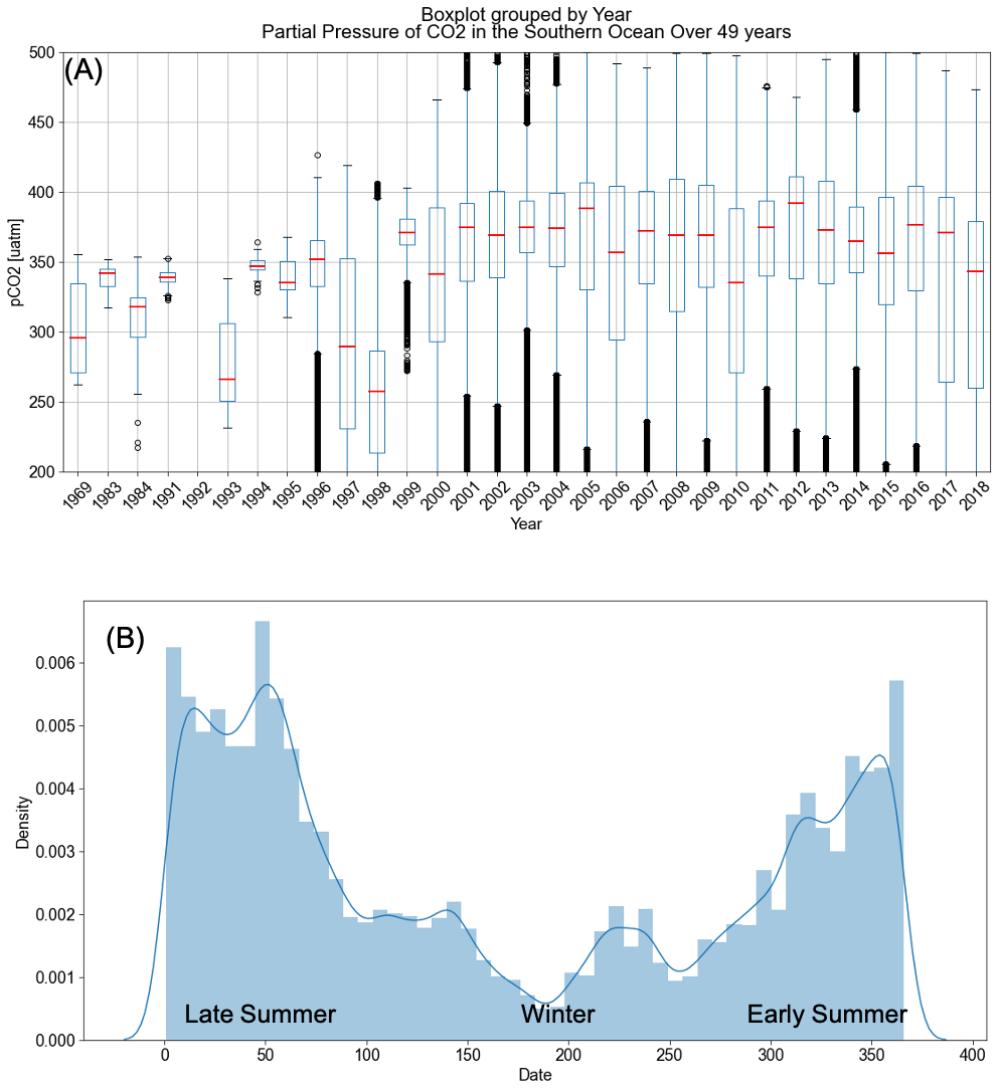

Figure 2:(a) Box and whisker plot showing the summary (median, minimum, and maximum pCO_2, Q 1 &2 and outliers) of pCO_2 data observed for each year for 49 years. (b) The seasonal distribution of the pCO_2 dataset binned by day of the year (x-axis).

Step 2: Interannual variability of pCO_2

The first approach assumes that the ice-covered region is uniform and therefore, the interannual variability of pCO_2 is regionally uniform. the interannual variability is considered (1) under ice, (2) in the different basins and (3) along the Goodhope Line. Three approaches have been carried out to understand and characterize the interannual variability of pCO_2 in the SIZ. Thus,

as a first investigation, pCO_2 was averaged spatially across the entire Southern Ocean SIZ for each year from 2000 to 2018. This approach assumes that the drivers of interannual variability are large-scale. The next approach recognizes that the interannual variability of pCO_2 may respond differently to regional drivers and, therefore, may be different across different ocean basins. To characterize any basin-wide differences in the interannual variability, in this approach, the seasonal subsampled data was spatially sorted into three different ocean basins (Atlantic, Pacific, and Indian) following basin definitions in Gregor et al. 2018. Lastly, we investigate the interannual variability of repeat transects of a single cruise line, the Goodhope Line (black box Fig. 1a). Here, apart from gridding the cruise transects onto the same 1-degree latitudinal grid using linear interpolation, no other spatial averaging is carried out, and thus any regional latitudinal difference per year can be explored.

Step 3: Regression analysis to provide insight into the interannual variability of primary drivers.

The monthly sea-ice and wind stress data were subsampled in time and spatially collocated to the observations. This allowed me to correlate the observational pCO_2 data with sea-ice concentrations and wind speed. Following Large, (1981), the co-located wind stress across was computed and correlated to the interannual pCO_2 variability across SIZ and different basins.

3.5 Decomposition of pCO_2

Following Takahashi et al. (2002), the pCO_2 was decomposed to its thermal and non-thermal components at each grid point (Eqs. 3.1-3.4) to determine which of the two drivers influences the surface ocean pCO_2 variability (Landschützer et al., 2015) of the Goodhope Line region.

$$1/ pCO_2 \, \partial pCO_2 / \partial T = \partial \mathrm{In} pCO_2 / \partial T = 0.0423 \, {}^{\circ}C^{-1} \quad 3.1$$

By normalizing the data to a constant temperature—the mean in situ SST depending on the focus taken into consideration—the thermal effect is eliminated from the observed pCO_2, as per Eq. (3.2).

$$pCO_2 \text{ at } SST_{mean} = (pCO_2)_{obs} \cdot \exp[0.0423 \cdot (SST_{mean} - SST_{obs})] \quad 3.2$$

In which pCO_2 represents the oceanic pCO_2. The subscripts "mean" and "obs" represent the average and observed pCO_2 and the mean of SST over the whole period, respectively.

By adjusting the mean pCO_2 with the variation between the mean and observed temperature, the impact of thermal fluctuations on pCO_2 has been calculated. The value of pCO_2 at a specific observed temperature (SSTobs) was computed using Eq. (3.3)

$$pCO_2 \text{ at } SST_{obs} = (pCO_2)_{mean} \cdot \exp[0.0423 \cdot (SSTobs - SSTmean)] \quad 3.3$$

The non-thermal factors are responsible for the residual variations in pCO_2 after the thermal effect is eliminated. The seasonal amplitude of pCO_2 values normalized to the mean SST, (pCO_2 at SSTmean), represents the non-thermal effects on the surface water pCO_2, (ΔpCO_2)n-T, using Eq.(3.4)

$$(\Delta pCO_2)n\text{-}T = (pCO_2, SST_{mean})_{max} - (pCO_2, SST_{mean})_{min} \quad 3.4$$

The seasonal amplitude of pCO_2 values normalized to the observed SST, (pCO_2 at SSTobs), represents the thermal effect of changes on the mean annual pCO_2 value, (ΔpCO_2) T.using Eq. (3.5)

$$(\Delta pCO_2)T = (pCO_2, SST_{obs})_{max} - (pCO_2, SST_{obs})_{min}. \quad 3.5$$

Chapter 4 **Results**

The interannual variability of SO surface pCO_2 is impacted by several drivers, as outlined in Section (1). These include SST (Kyle C Armour and Cecilia M Bitz, 2015); (Fassbender et al., 2018; Williams et al., 2018); sea surface salinity (SSS), sea-ice concentration (Moreau et al., 2016), and wind stress (Keppler & Landschützer. 2019). Changes in these drivers may manifest from large-scale changes in the SAM (Doddridge & Marshall, 2017; Keppler & Landschützer, 2019; Lee et al., 2019; Lefebvre et al., 2004; Simpkins et al., 2012). In this section, I investigate how changes in SSS, SST, winds, and sea-ice concentration impact pCO_2 variability in the SIZ, a largely understudied region of the Southern Ocean.

The results are arranged into three subsections ranging from SO-wide SIZ analysis to inter-cruise-specific analysis (sections 4.1 to 4.3). Section 4.1 compares the SO SIZ pCO_2's interannual variability and its correlation with SST, SSS, wind speed, sea-ice concentration, and the SAM index. Section 4.2 investigates whether the results shown in 4.1 are sensitive to the basin-scale variability of these drivers by comparing the interannual variability of pCO_2 averaged across the Atlantic, Indian, and Pacific basins. Section 4.3 uses repeat cruise transects to investigate specifically the role of thermal and nonthermal components of pCO_2 on the latitudinal distribution of pCO_2 along the Goodhope Line.

4.1 Interannual variability of pCO_2 in the seasonal ice zone of the Southern Ocean

The time-series of summer mean (DFJ) surface ocean pCO_2 obtained from all SOCAT measurements and spatially averaged south of the 50˚S (i.e., encompassing the SIZ, Fig 1a) are shown in Fig. 3a. Uncertainty estimates are provided as the standard error of the mean to represent the summertime variability of pCO_2. A significant standard error shows how representative the mean is compared to observations. It also indicates that the uncertainty associated with the mean is significant; however, in this regard, the standard error for pCO_2

and drivers (Fig. 3b-f) is low compared to the inter-summer differences of the mean pCO_2. Therefore, the bias associated with the number of observations taken in an exceptionally high or low pCO_2 region for a given year does not significantly impact the inter-annual variability of the mean summer pCO_2. The corresponding (e.g., collocated in space and time with SOCAT pCO_2) drivers, SST, SSS, sea-ice concentration, wind speed, and SAM are shown in Fig. 3b-f. The year-to-year range of pCO_2 in the SIZ from 2000 to 2018 has a minimum pCO_2 of 290 µatm in 2004 and a maximum pCO_2 of 355 µatm in 2003. From 2000 to 2004, similar modes of variability of pCO_2 are reflected in some of the drivers, particularly in salinity and sea-ice concentration, which appear slightly lagged (Fig. 3a and e). While the interannual variations in pCO_2 do not correspond to the interannual variations in the SAM index (Fig. 3a, f), there are some indications that the SAM could potentially play a role in longer mode time scales (decadal). For example, the SAM index tends towards a more positive phase from 2004 until 2016, coinciding when pCO_2 starts its slow decadal increase from 290 to 350 µatm. This period coincides with the CO_2 uptake "reinvigoration" period identified by Landschutzer et al. 2016, which has been linked to a tendency towards zonally more asymmetric atmospheric circulation. Fig. 3e shows that from 2002 to 2016, the mean wind speed increased from 2.51 to 5.1 m. s^{-1} as the SAM index moves towards the positive phase, although the interannual variability of the mean wind speed can be of the same order as the trend. Fig. 3c & d highlight the interannual changes in salinity and sea-ice concentration, increasing from 33.3 to 34.0 PSU and 10% – 50%, respectively. The inter-annual co-variability between summer mean SSS and sea-ice concentration are primarily out of phase, with years of freshening associated with less sea-ice concentration.

Notably, from 2016, there was a rapid decline in collocated sea-ice (Fig. 3d); this decline is documented by several studies as a widespread rapid decrease in sea-ice (refer to Fig. 3c from Parkinson, 2019). This reduction of sea ice has been linked to an increasingly wave-3-like structure of the SAM (Schossler et al., 2020). Here we note a significant change in the SAM index over this period (Fig. 3f) along with an increase in wind speed. The response time of SST, SSS, sea ice, and pCO_2 to wind forcing are all within one year. Interestingly, in response to this decline in sea-ice, there is a decrease in pCO_2 over this period. This is evidence that

processes that force the ocean on seasonal time scales are important for setting its interannual variability.

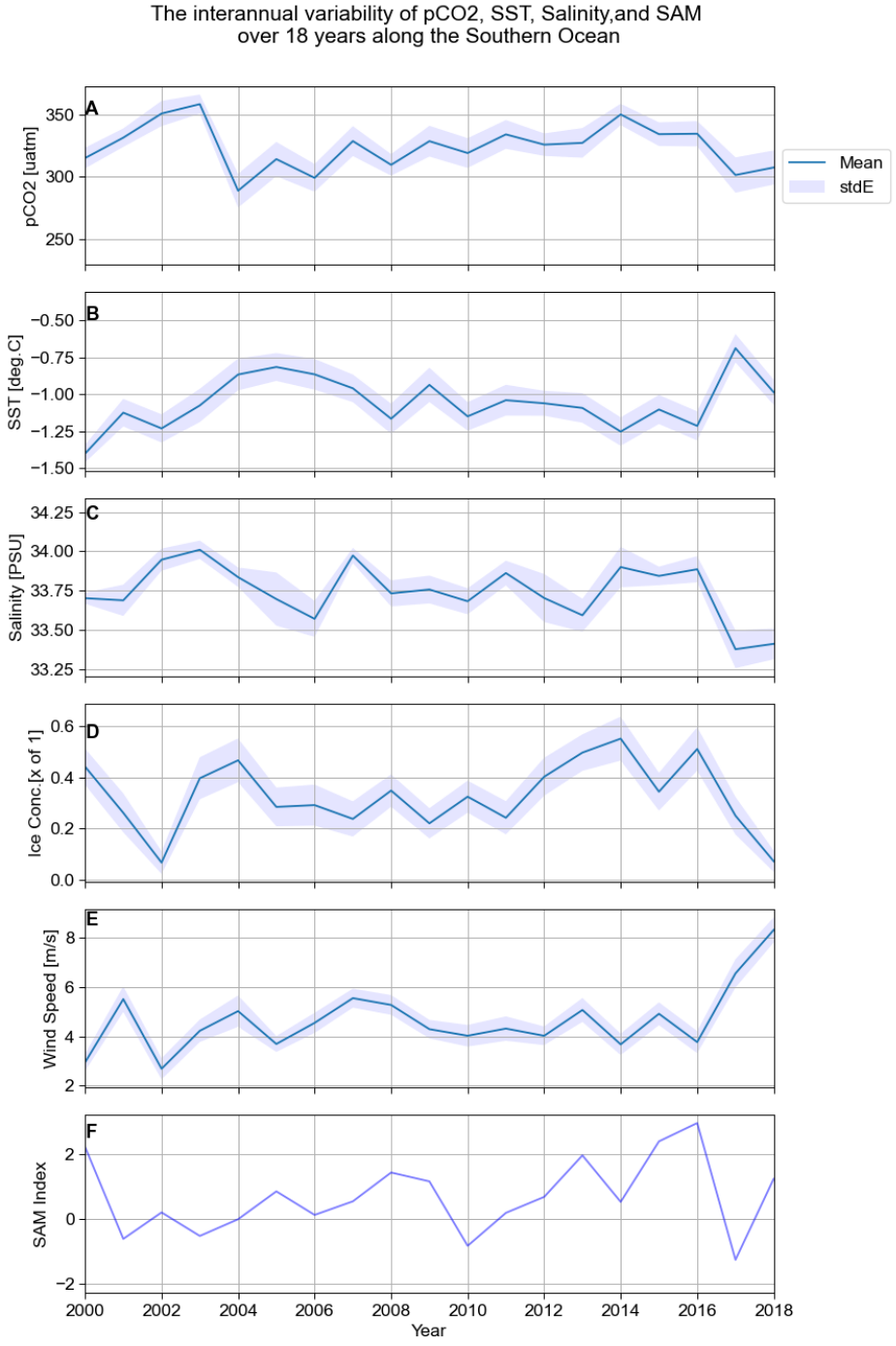

Figure 3: The Southern Ocean year-to-year DJF mean and standard error (shaded along the mean) of (A) pCO_2 (µatm),(B) sea surface temperature (°C), salinity (PSU), maximum sea-ice concentration (0 to 1), and Wind speed (m s-1) from 2000 to 2018.

The correlation matrix in Fig. 4 summarises the correlations between the summer mean of the various drivers (shown in Fig. 3b-f) with pCO_2. pCO_2 value obtains a negative correction with SST (i.e., r = -0.68 and r^2 = 0.46) and positively correlates with SSS (r = 0.67, r^2 =0.45). This implies that variations in SST and SSS are linked to changes in pCO_2 and its interannual variability in the SIZ. When SST increases, fresh water is introduced, likely through increased sea-ice melt, decreasing salinity (density), low solubility CO_2, and, in turn, reducing pCO_2 due to the thermal response. Moreover, some nuances than the direct link to temperature (and decreased solubility of CO_2) contribute towards the reduction of pCO_2.Freshwater stratification introduces stable conditions for enhanced biological production, potentially decreasing the surface pCO_2.

There was no/weak correlation between SAM and pCO_2 (r = 0.12 and r^2 = 0.01) and between pCO_2 and sea-ice concentration (r = 0.01 and r^2= 0.01). It is plausible that this low correlation can be attributed to the lagged system-scale response of the SAM or the regional (basin-scale) positive and negative responses to SAM- due to the opposing effects of enhanced outgassing in upwelling regions and enhanced carbon uptake elsewhere (e.g., Prend et al., 2022; Sallée et al., 2010), thus, resulting in the increasing trend towards more asymmetry in the SAM that is driving a non-zero mean. It is also plausible that this low correlation is a result of multiple cascading complex responses (both physical and biological) to the SAM which impact pCO_2 antagonistically. According to previous studies conducted in the Southern Ocean, positive SAM phases correlate with anomalous outgassing in the region between ~50°S and ~65°S, except for in the Atlantic sector due to anomalous uptake of anthropogenic CO_2 (Keppler & Landschützer, 2019; Landschützer et al., 2016; Prend et al., 2022). This shows a lack of uniformity in the SAM response across the Southern Ocean. The zonal asymmetry of the SAM does not reflect the regional variability of pCO_2, but instead, it depicts the interannual and decadal variability due to the spatial average index used across the entire SO, therefore giving ground to investigate the strength of the relationship between the primary drivers and pCO_2 in the different ocean basins.

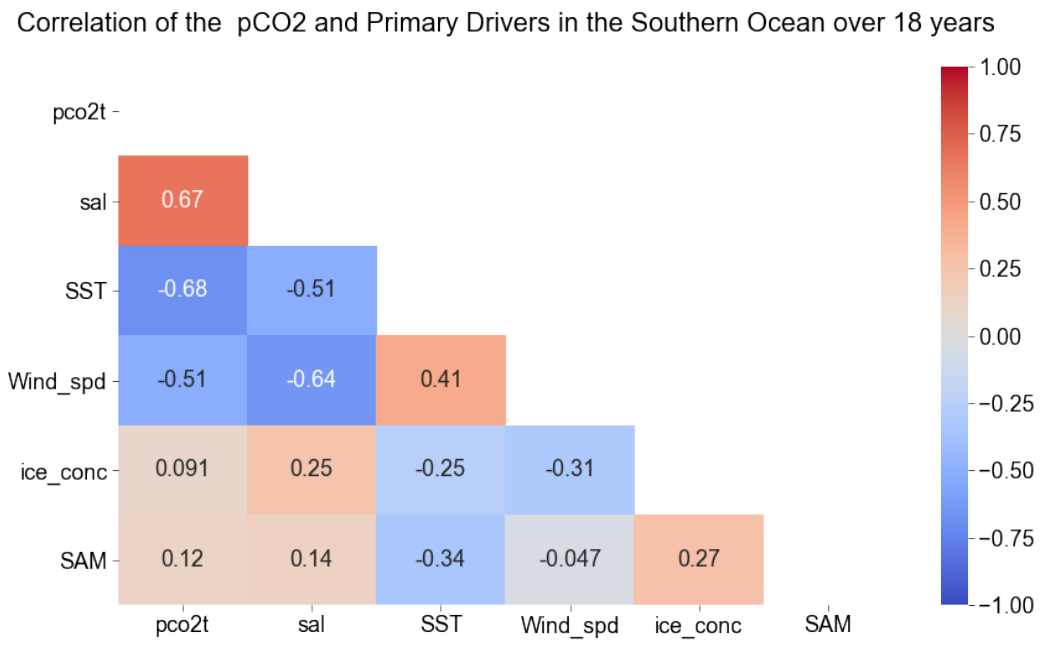

Figure 4: The Correlation matrix of pCO_2 with primary drivers (salinity, sea surface temperature, wind speed, and sea-ice concentration) and SAM in the Southern Ocean over 18 years (2000-2018).

4.2 Basin-scale drivers of interannual variability of pCO_2 in the seasonal ice zone

The Southern Ocean comprises different zonal sectors that are highly dynamic. Fig. 5a illustrates the three major ocean basins in the Southern Ocean –the Atlantic, the Indian, and the Pacific. The different sectors have unique dynamics, which influence the interannual variability of pCO_2. To gain a more comprehensive understanding of the primary drivers of the interannual variability of pCO_2 within each basin, a correlation between each primary driver and pCO_2 is determined. The results shown in Fig. 5b-d indicate that pCO_2 remains weakly correlated to the SAM in all three basins ($r = 0.093$, $r = -0.36$, $r = 0.25$ for the Atlantic, Indian, and Pacific, respectively), there is a strengthening in the correlation in the Pacific and Indian Oceans, compared to the Southern Ocean wide average ($r = 0.12$). Noticeably, the correlation between pCO_2 and SAM for the Atlantic and the Pacific Oceans is positive, while there is a negative correlation in the Indian Ocean. This suggests the presence of the opposing

responses of the SAM between the basins, as mentioned previously. Several studies (Fogt & Marshall, 2020; Keppler & Landschützer, 2019; Lenton & Matear, 2007) have indicated that the SAM index is based on the spatial average of the entire SO hence only interannual and decadal variability is observed. These studies correlate CO_2 flux with SAM in different basins (positive SAM correlation in both the Pacific and Indian Oceans and a negative SAM collation in the Atlantic Ocean) instead of a regression between SAM and pCO_2. The separation into basins has further revealed the robust regression between pCO_2 and salinity. The correlation matrix suggests that salinity is a dominant driver for interannual changes in pCO_2. The Atlantic Ocean has the highest positive correlation of $r = 0.87$ ($r^2 = 0.75$), followed by the Indian and the Pacific Oceans, with a correlation of $r = 0.59$ and $r = 0.48$, respectively. Salinity is anti-correlated to SST in both the Pacific and Atlantic basins, indicating that the low salt concentration is in the seawater when SST is high, suggesting sea melt as a key driver in the interannual changes of salinity and thus pCO_2.

Importantly, both the SIZ-wide (Fig. 3) and basin-scale separated averages of pCO_2 (Fig. 5) may be impacted by the yearly varying spatial and temporal distribution of the sampling performed by ships and other platforms incorporated into SOCAT. For example, more sampling in the Drake Passage versus the region within the Atlantic Ocean (GoodHope Line) in a particular year could result in different pCO_2 values due to the different regions being sampled. To reduce such biases and gain a deeper understanding of the influence of salinity and other drivers on the sea surface pCO_2 in the Atlantic Ocean, I investigate repeat (annual) ship transects along the Goodhope Line, which measured the latitudinal distribution of pCO_2 along with the primary drivers.

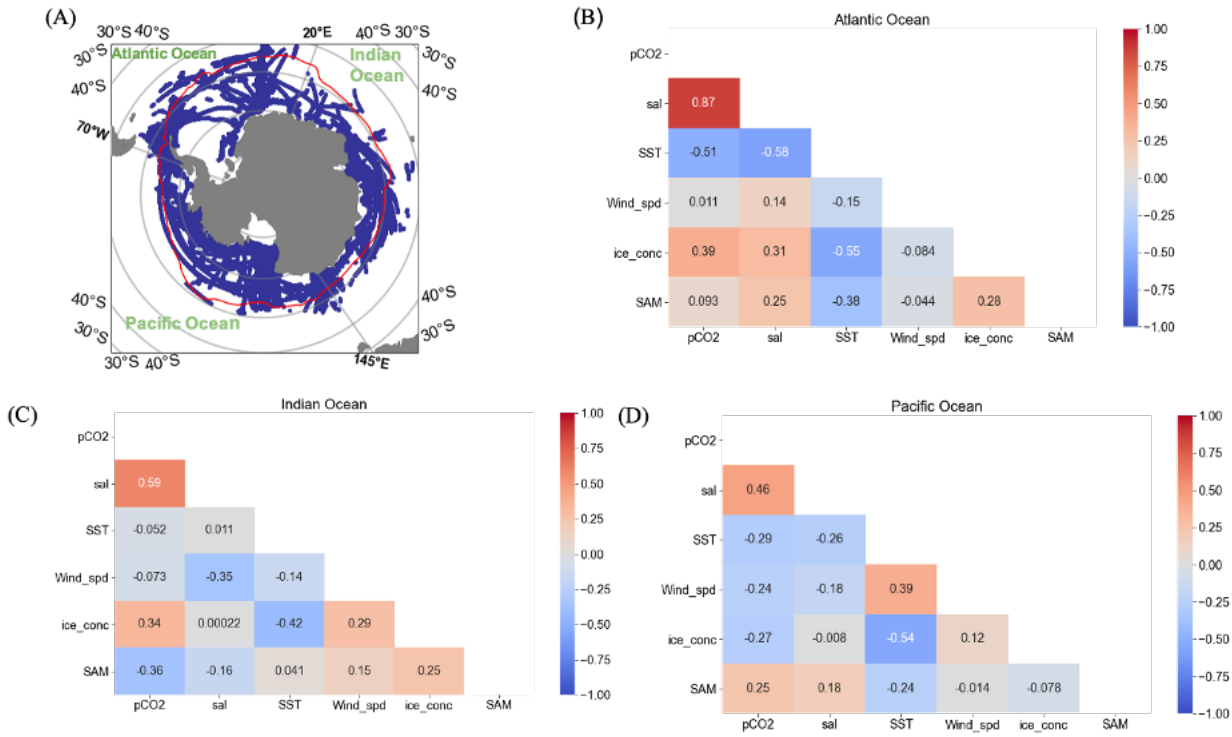

Figure 5: A) A map of three ocean basins in the Southern Ocean, illustrating the Atlantic (70° W - 20° E), Indian (20° E - 145° E), and Pacific Ocean (145° E - 70° E) along with the maximum sea-ice concentration (red line). The correlation of the primary drivers (Sea surface salinity, sea surface temperature, sea-ice wind, and sea-ice concentration) and pCO_2 in the (B) Atlantic, (C) Indian, and (D) Pacific Oceans over 18 years.

4.3 Interannual variations of pCO_2 and the drivers along the Goodhope Line

4.3.1 Spatial and temporal distribution of pCO_2 along the Goodhope Line

The location of the yearly repeated cruises/ship transects along the Goodhope Line and the total number of pCO_2 observations made per year from 2002 to 2016 are shown in Fig. 6a, b. About 20,000 pCO_2 observations were reported in 2002, followed by a four-year gap in observations until 2006. The number of pCO_2 observations made between 2007 and 2016 was relatively consistent (2000 to 8000, apart from in 2014 when there were about 18,000 observations), thus allowing for the investigation of the interannual variability of pCO_2. The

latitudinal distribution of pCO_2 measured from the repeat cruises is illustrated in Fig. 6c. There is a general meridional pattern, where at the lower latitudes that are closer to where the SIZ meets the open-ocean (52° S to 60° S), the range of annual observed pCO_2 values is about five times smaller (340 - 380 µatm) compared to the range (240-430 µatm) measured closer to the ice shelf (61° S to 70° S), where measured pCO_2 is widely distributed between years. Thus, the interannual variability appears sensitive to the process occurring at these different latitudes and is stronger further south. Therefore, the question arises: What could be driving this latitudinal variation in the observed interannual spread/variability of pCO_2 data?

To investigate this further, I first explore whether this spread is an artifact of sampling biases. In other words, can this wide distribution in the observed pCO_2 be attributed to the time (e.g., different months) at which the annual observations shown in Fig. 6c were recorded? The pCO_2 measurements at high latitudes might have been recorded during early summer, and those closer to the ice shelf were recorded during late summer.

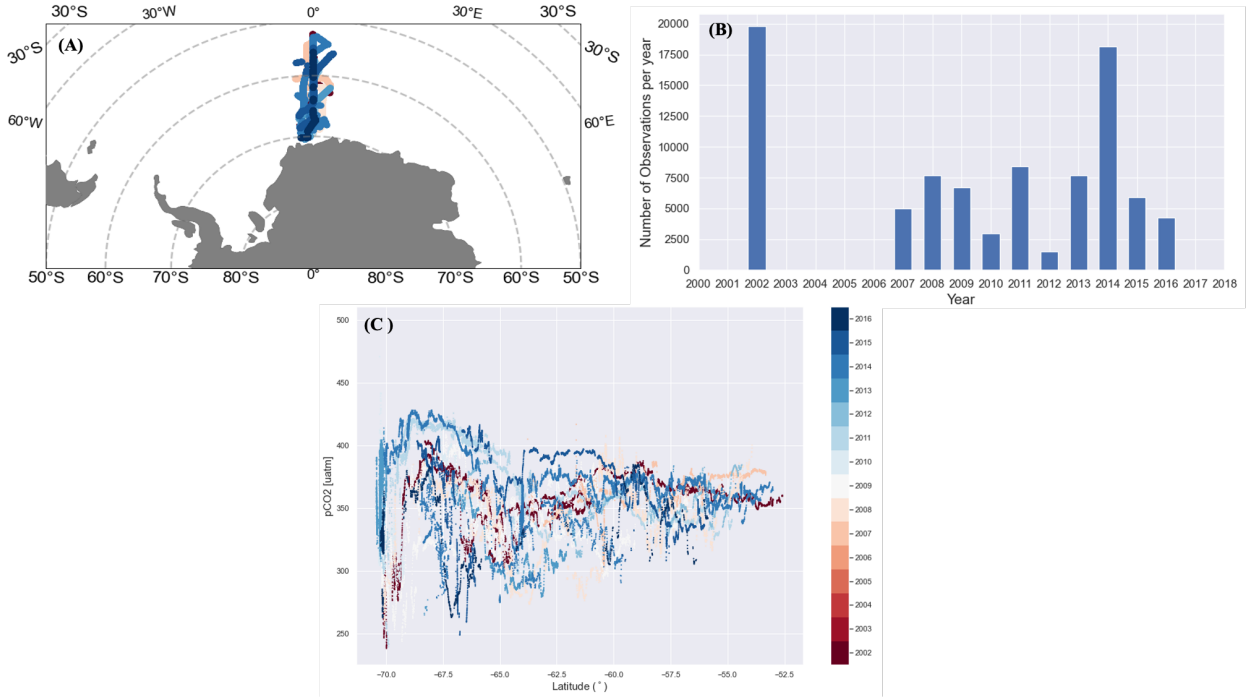

Figure 6: (a) The repeat cruises along the Goodhope line, (b) the number of pCO_2 observations per year from 2002 to 2016, and (c) the longitudinal distribution of pCO_2 (µatm) for the repeat cruises with a colour bar that corresponds to the colour of the cruises in (a).

To investigate this further, Fig. 7a shows the temporal distribution of the pCO_2 observations from summer. It highlights the number of observations made in both early and late summer. Late and early summer pCO_2 observations are between 0-to-100 year-days (January to February) and 300-to-365 (November and December) year-days, respectively. The high number of pCO_2 observations made during early summer is highlighted in Fig. 6a. The pCO_2 measurements made in early summer have a typically higher pCO_2 (mean of ~358 µatm) compared to those in late summer (mean of ~304 µatm) (Fig. 7b), as similarly seen in the literature. For example, Fig. 7 from Williams et al. (2018) shows that the summer difference between early and late summer in the SIZ could be as significant as 51 µatm (395 µatm in early summer and 344 µatm in late summer). Fig. 7b shows the latitudinal distribution of pCO_2 as in Fig. 6c but is marked by the month that the observation was carried out. pCO_2 observations between 50.5 °S to 60 °S, with the narrower interannual range of pCO_2, coincided with mostly observations carried out during early summer (December, Fig. 7b). The more extensive spread of the interannual pCO_2 further south (south of 60°S) towards the ice shelf detailed observations carried out across all three months. In this region, the magnitude

of pCO_2 during early summer is higher (mean of ~367 µatm) than during late summer (mean of ~343 µatm). Thus, it is plausible that sampling different times of the summer season may have somewhat contributed to this more extensive spread in interannual variability further south (Fig. 5c, Fig. 6b) rather than a driver, such as more considerable interannual changes in salinity in the south than in the north. Nevertheless, there still appears to be more variation in, for example, January moving from the open ocean into the ice zone (Fig. 7b). Thus, while I do not completely rule out the possibility that the SIZ, a highly dynamic region, could have strong interannual variations compared to the open ocean, the point here is to illuminate possible misleading interannual variations due to sample bias.

In the preceding section, 4.2, I showed that the large-scale pCO_2 in the Atlantic basin strongly correlates to salinity. This correlation was determined with all the data found within the basin. However, the sparsity of data in the basin results in challenges in determining the correlation between local-scale pCO_2 and salinity. This implies that the correlation between large-scale pCO_2 and salinity may not represent the relationship between local-scale pCO_2 and salinity. Therefore, I will investigate possible drivers that may influence pCO_2 and determine whether the local-scale pCO_2 is strongly linked to salinity.

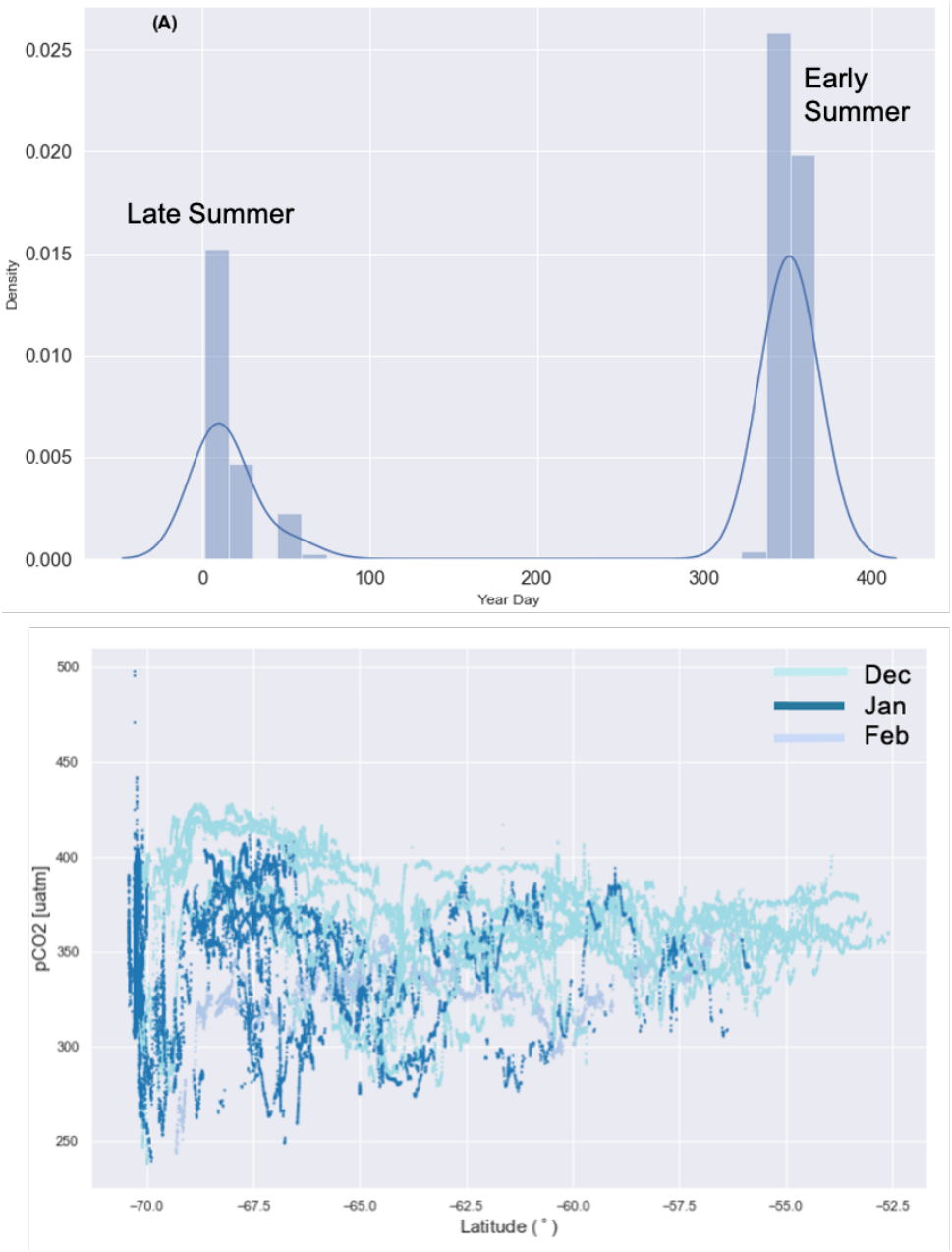

Figure 7:(a) The year-day density plot showing the distribution of summer pCO_2 observations made in the early (Dec) and late summer periods (Jan - Feb), (b) the latitudinal distribution of the early and late summer pCO_2 (µatm) observations.

4.3.2 The primary drivers of pCO_2 variability along the Goodhope Line

The Goodhope Line transect is determined here as all observations within 5 °E – 5 °W. A significant source of these observations is from repeat cruises between Cape Town and Antarctica. This transect goes beyond the established boundary. Therefore, several observations made on this transect fall out of the boundary. This results in incomplete data observations along the transect. Only nine cruises with complete observations between 55°S and 70°S are re-gridded and used to investigate spatial variability between various cruises to overcome this bias (Fig. 8). At lower latitudes (55-58˚S), the interannual pCO_2 values (Fig. 8d) are closely grouped and ranging between 340 – 390 µatm, while at high latitudes (65-70˚S), the interannual pCO_2 spread out ranges between 250 – 440 µatm. As also noted previously, there is a slight tendency (on average, refer to bold black line) for pCO_2 to be higher in the south into the sea-ice zone and lower in the north into the open ocean. Additionally, this figure illustrates the latitudinal distribution of selected drivers (SST, salinity, density) as well as the decomposition of pCO_2 into the thermal and non-thermal components (refer to eq. 3.1 – 3.2 described in the methods section) for nine cruises (Fig. 6a – b).

As expected, the SST observed in Fig. 8a shows that lower latitudes (from 55 °S to 57 °S) have higher SST, ranging from -1.7° C to 0.0° C compared to higher latitudes (from 67 °S to 70 °S) with low SST ranging from -2.1° C to – 0.8 ° C. The mean latitudinal distribution (black line) of SST changes from high (~ - 0.7° C) in low latitudes to low (~ - 1.5° C) in high latitudes. Fig. 8b, c shows that salinity and density values are low at lower latitudes, with ranges of 33.5–34.2 PSU and 1023.4 – 1026.8 $kg.m^{-3}$, respectively. At high latitudes, salinity and density were both larger, ranging between 33.9 – 34.2 PSU and 1027.1 – 1027.5. $kg.m^{-3}$, respectively. With high latitudes, SST decreases while salinity and density increase. The observed southward increase in SSS may be due to several factors, such as brine rejection further south during sea-ice formation, the northward transport of low-saline ice-melt water, and the outcropping of high-saline UCDW in the south (e.g., see Fig. 1 in Haumann et al., 2016). The thermal and non-thermal decompositions of pCO_2 are shown in Fig. 8e, f. The thermal component of the pCO_2 range (-10 – 19 µatm) is suppressed compared to the non-thermal pCO_2 range (-90 – 100

µatm), which is on the order of magnitude of observed fluctuations in pCO_2.The variability in non-thermal pCO_2 matches the modes of variability observed in the pCO_2. This shows that non-thermal drivers of pCO_2, such as those linked to changes in DIC, alkalinity, and salinity, are dominant drivers of the pCO_2 variability over the interannual changes in SST in the SIZ.

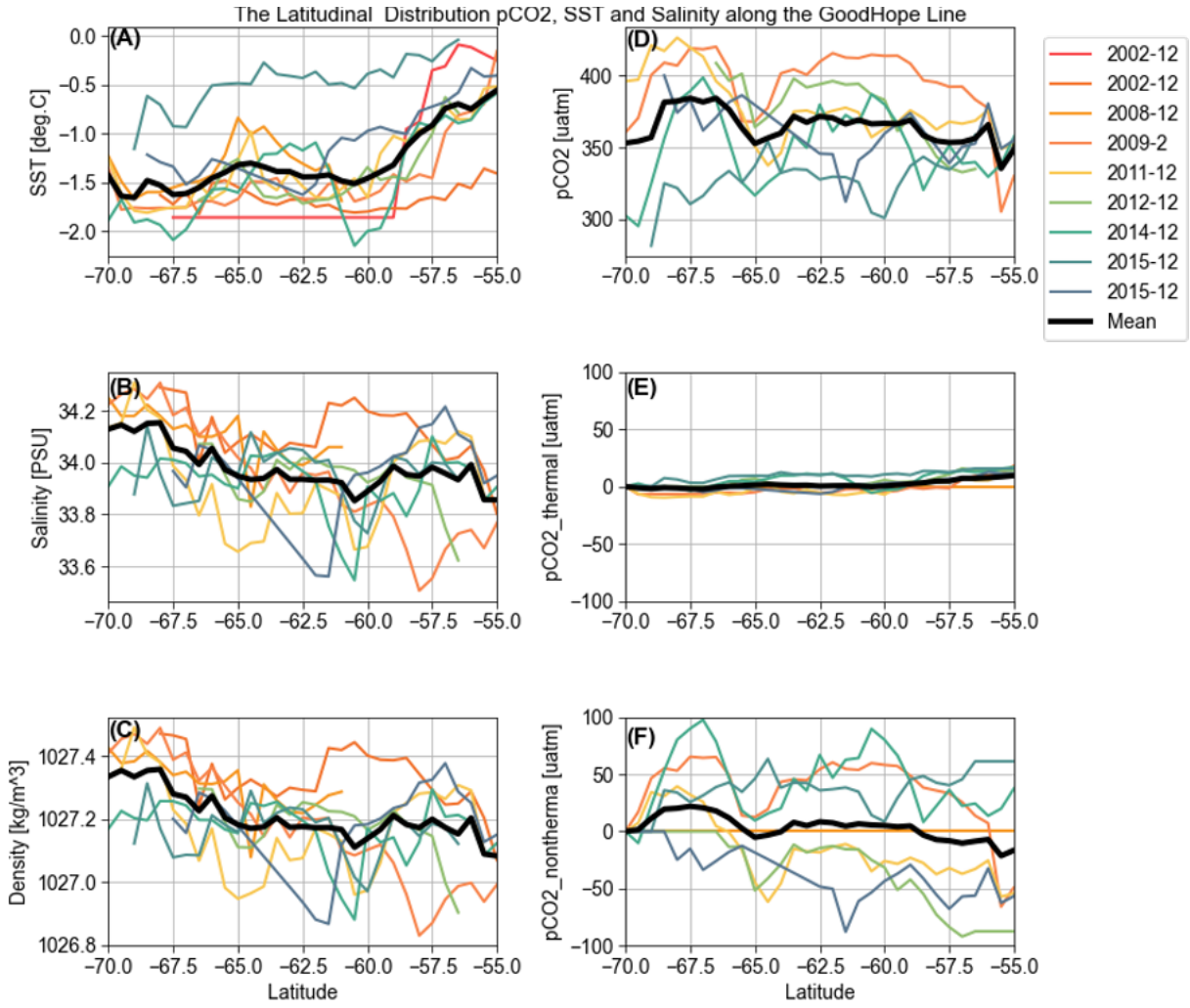

Figure 8: (a) The latitudinal distribution of pCO_2 and drivers, which includes (a) SST (°C), (b) salinity (PSU), (c) density (kg.m-3), (d) pCO_2 (µatm), and the (e) thermal and (f) non-thermal components of pCO_2 (µatm). The latitudinal distribution mean of each variable is represented by a black line for nine cruises along the GoodHope Line.

Chapter 5 **Discussion**

This study investigates the summer-time interannual variability of sea surface pCO_2 in the sea-ice-impacted SO and its potential drivers. This region needs to be studied more due to the sparsity of observations. However, the recent increase in the number of research and resupply voyages entering the SIZ and the collation and quality control of these pCO_2 data by SOCAT offered an opportunity to explore this further. In this thesis, I conduct three levels of investigations on pCO_2 interannual variability, (1) a large-scale SIZ-wide averaged approach, (2) a basin-scale averaged approach, and (3) a local-scale approach through interannual comparison of individual cruise tracks along the Goodhope Line. Here, I discuss this study's key drivers, sampling aliasing, and limitations.

5.1 Drivers of interannual pCO_2 variability in the seasonal ice zone

In general, the changes in surface ocean pCO_2 are known to be driven by CO_2 production/consumption due to biological activities, lateral and vertical advection, dilution by sea-ice/glacial meltwaters, temperature changes, and mixing with ambient water masses (Arroyo et al., 2019; Legge et al., 2017; Shadwick et al., 2021). Importantly, I have elected not to include biological production as a driver in this thesis, not because it is not a key candidate but simply due to the limited observations in the ice region (e.g., not available from SOCAT and not easily constrained in this region from satellite).

In the SIZ-wide averaged approach, it is difficult to disentangle the drivers of interannual variability likely due to different and/or opposing physical-biogeochemical properties of each basin and the regionally diverse responses to wind forcing (Fig. 4). However, links between SAM and pCO_2 become more apparent on longer multi-annual-scale time-scales (years 2002-2012, Fig. 3) as similarly noted by several studies (DeVries, 2017; Gruber et al., 2018; Keppler & Landschützer, 2019; Lovenduski et al., 2007; Lovenduski & Gruber, 2005; Ritter et al., 2017). Despite the weaker trend observed in the 2000s, pCO_2 has been increasing year by year (Fig.

3a). This increase in oceanic pCO_2 in the SIZ coincides with the reinvigoration period of air-sea CO_2 fluxes period (Gruber et al., 2018; Keppler & Landschützer, 2019; Landschützer et al., 2015). All three sectors of the Southern Ocean are contributing to the resurgence of the carbon sink, but process differences exist between sectors. Landschützer et al.,(2015) proposed mechanism is a zonally asymmetric atmospheric circulation resulting in a dipole of ocean warming and cooling, which led to the Southern Ocean reinvigoration period (2002 - 2011). This zonally asymmetric mechanism does substantiate the low correlation between SAM and the pCO_2 and between pCO_2 and ice concentration when averaging across the entire Southern Ocean SIZ (Figures 3 and 4). Another study by Gregor et al., (2018) argues that the interannual drivers of the Southern Ocean's carbon sink are seasonally decoupled, with wind stress and biology being the main drivers in Austral winter and summers, respectively. The large decadal variation of the Southern Ocean carbon sink suggests a rather dynamic ocean carbon cycle that varies more in time than previously recognized.

A notable exception to the lack of association between pCO_2 and drivers on interannual time scales can be seen from 2016 onwards (Fig 3). Here, a sudden and intense change in the atmospheric forcing (SAM) was associated with stronger winds and a rapid decline of sea-ice. And in this case, an immediate response to the pCO_2. This rapid decline of sea ice is broadly attributed to the shift in regression patterns between sea-ice and SAM which is likely linked to an increasingly wave-3-like structure of the SAM (Schossler et al., 2020). This decline in sea-ice has continued beyond the time reported by this study (2.1×10^6 km^2 in 2017 km^2 to 1.92×10^6 km^2 in 2022) (Holland et al., 2017; Turner et al., 2022). Thus, future work should include all available data to date to explore the response of pCO_2 and ultimately to understand how such critical ice-loss events (which may be on the increase according to Turner et al., (2022) may be impacting CO_2 fluxes on global scales.

In the basin-scale averaged approach, a strong relationship between salinity and pCO_2 emerged, particularly in the Atlantic (Fig. 5). This highlights the important links between interannual variability in sea-ice, sea-ice freshwater melt, and pCO_2 at these basin scales. It also highlighted the regional diverse responses to forcing (SAM and pCO_2 have different, albeit weak, correlation signs in different basins). The increase in SST from winter to summer

creates an inflow of freshwater from melting sea-ice, therefore diluting the brine concentration on the sea surface and decreasing SSS. The reduction in SSS impacts the dissolution of CO_2 which could explain the resulting changes in pCO_2. Moreover, the increase in meltwater may increase upper ocean stratification, resulting in reduced vertical fluxes of dissolved inorganic carbon from the carbon-rich CDW and potentially increased primary production (I. Giddy et al., 2021; I. S. Giddy et al., 2023) which could both lower oceanic pCO_2. The relationship between pCO_2 and salinity could be stronger in the Atlantic basin due to having higher SSS (Weddell Gyre is a significant sea ice production region) than both the Pacific and Indian basins in all latitudes (Fig. 4). This is thought to be associated with the Atlantic Meridional Overturning Circulation and deep-water formation (which affects the interannual variability of pCO_2) in the high-latitude North Atlantic (Craig et al., 2017). The results of this study provide further evidence that there is a relationship between salinity and pCO_2, which can be considered when studying the importance of the SSS and sea ice relationship using model-based analysis.

Finally, the local-scale approach (analysis of repeat cruise transects), provided further insights into latitudinal variations in the interannual variability of pCO_2 in the Atlantic Southern Ocean (Fig 7-8). The interannual variability of pCO_2 increases in magnitude further south into the SIZ when moving away from the boundary of the SIZ and the open ocean. This is apparent even when considering possible sampling biases due to sampling in different seasons (Fig 7b). Kimura et al., (2023) have indicated that in addition to seasonal variability, the Antarctic sea-ice extent also varies on multiple time scales, ranging from daily intra-seasonal, interannual, and multi-decadal time scales. It is important not to only focus on the local scales of sea ice but also to understand processes that influence the change in sea ice in various time scales. In general, sea ice extent changes through both thermodynamic and dynamic processes. Thermodynamic processes include sea ice formation and melting, while dynamic processes include ice transport and ice deformation (e.g., raft formation and ice wave formation). These processes can be used to determine regional differences in the process of the seasonal and interannual changes of ice area and the location (marginal ice zone and ice area) where the difference processes occur. This approach will not also help differentiate between seasonal and interannual variability, but also thermal and non-thermal drivers of the processes

involved. The interannual variability of pCO_2 along the Goodhope Line is primarily driven by non-thermal drivers, which include SSS, DIC, and primary production. However, the main non-thermal driver of pCO_2, along with its magnitude, is not explored here. To determine which of the non-thermal drivers is responsible for pCO_2 variability requires additional analysis to separate and quantify the potential drivers, this is left for future work. According to Jersild & Ito, (2020), for the Drake passage repeat transects, there is a robust biological drawdown of CO_2 during the late spring and early summer months, resulting from the minimum surface DIC and pCO_2.

5.2 The effects of regional and temporal sample aliasing and limitations on the interannual variability of CO_2

It is important to recognize the potential for the propagation of temporal and spatial aliasing to influence the mean and thus results presented in this study. The results of this study show intra-seasonal (between early and late summer) and interannual variability, with more pCO_2 observations during the early summer over 18 years (Fig.7). During early summer, the number of pCO_2 observations is high as the ship moves towards the SIZ due to the duration of the trip (more ice) and lower when the ship returns (less ice). In contrast, during late summer, some pCO_2 observations are integrated into the early winter pCO_2 observations. This integration is reflected in the magnitude of pCO_2 measurements made between early summer and late summer. The inconstancy in the number of intra-seasonal pCO_2 observations yearly may impact the representation of interannual variability of pCO_2. Due to the remoteness and harsh climate conditions, the number of voyages varies from one year to the next, therefore creating an inconsistency in pCO_2 observations. This inconsistency creates both spatial coverage and temporal resolution limitations that may result in biased computation and quantification of the magnitude of interannual variability of pCO_2.

In this study, the data collection platform consists of restricted data from specific regions within the Southern Ocean. The pCO_2 observations in these regions are captured due to the

repeat Southern Ocean voyages. Amongst these regions, some are under-sampled due to the remoteness and harsh conditions of the Southern Ocean, thus causing a spatial coverage limitation, and temporal resolution is also affected. The amount of pCO_2 observations in these regions varies from year to year, therefore the SO-wide interannual variability of pCO_2 is misrepresented. Furthermore, the restrictive basin definitions used in this study also emphasize the spatial coverage limitation. The basins were defined based on geographic boundaries instead of dynamic regions such as the Drake Passage and the Weddell Sea. The geographical boundaries include the major activity areas and under-sampled regions, influencing the mean pCO_2 observed within each basin. For instance, the Drake Passage is located between the Atlantic and Pacific oceans; thus, the geographic boundary divides this region into two oceans. This then affects the data collected in this region, implicating the separation of the data between the two basins, resulting in incomplete pCO_2 observations. In addition, various regions within each basin are under-sampled. The inconsistency of pCO_2 observations lowers the overall pCO_2 mean in each basin.

A feasible approach to overcome the bias/limitations associated with geographic boundaries would be to focus on dynamic regions such as the Drake Passage and the Weddell Sea. These regions are well sampled and are the central regions influencing the pCO_2 distributions in the entire basins. For instance, the Drake Passage has one unique time series amongst the Southern Ocean research programs in both partial and temporal coverage. High-frequency underway observations of the surface ocean partial pressure of CO_2 (pCO_2 comments are made by Antarctic Research and Supply Vessel Laurence M. Gould) (Lovenduski et al., 2007; Munro et al., 2015). In addition, spatial and temporal resolution limitations can be reduced by using observational platforms such as Lagrangian drifting buoys and Argo floats to constrain the basin-scale mean seasonal cycle and provide the potential role of fine-scale dynamics (Boutin et al., 2008; Resplandy et al., 2014).

It is evident that ship-based observations are helpful; however, more is needed to resolve the seasonal cycle due to the operational limitations of the required sampling frequency. Amongst others, this regional and temporal sample aliasing of pCO_2 is a significant issue that presents challenges in studying the interannual variability and trends of sea-air CO_2 flux

(Djeutchouang et al., 2022; Fay & McKinley, 2017; Landschützer et al., 2014; Majkut et al., 2014; Monteiro et al., 2015). It may cause substantial uncertainty in the mean CO_2 flux, as aliasing may result in the exclusion of short-scale (temporal and spatial) signals that may be important for driving changes on longer and larger scales. As such, the decadal variability of CO_2 flux, as discussed in this study, is already under question because of spatio-temporal aliasing (Hauck et al. 2023).

Finally, an additional limitation of this study is the use of the SAM index rather than pressure fields. The SAM index is based on a spatial average of the entire SO hence it can show both interannual and decadal variability/trends. Using the SAM index for regional correlations (basin-scale) creates issues with its inability to detect nuances in the range of SAM asymmetries associated with the different regions. To determine the regional correlation, a similar approach to that of Elio Campitelli, (2022) can be employed. Whereby, the zonal asymmetry and symmetry components of the SAM variability and their impact are determined using monthly regression geopotential height fields at each level. This exploration is left for future work.

Chapter 6 **Conclusion**

The Southern Ocean is notoriously under-sampled due to its remoteness, thus establishing biases and limitations associated with the quantification of pCO_2 and its potential drivers. This study aimed to investigate the interannual variability of pCO_2 along the SIZ during the austral summer season. Ship-based observational data obtained from the SOCAT data platform was used and interpolated to summer months over 18 years. The data was then divided into three categories, which are (1) the large-scale Southern Ocean-wide (2) 3 basin scales (Atlantic, Pacific, and Indian Ocean), and (3) the Goodhope Line. The interannual mean variability for pCO_2, the potential drivers (ice concentration, wind, SSS, SST, and SAM), and the correlation matrix for all three divisions. Based on these analyses, it was difficult to determine the drivers of the large-scale SO-wide interannual variability of pCO_2 in the SIZ due to the physical-biogeochemical properties of each basin and the regional-diverse responses to wind forcing, which also influences the relationship between SAM and pCO_2. The link between SAM and pCO_2 is more apparent on longer decadal-scale time scales. Noticeably, on a basin scale a strong relationship between salinity and pCO_2, particularly in the Atlantic Ocean, highlighting the link between variability in sea ice, freshwater, and pCO_2. It has also been determined that the repeat cruise transects highlight that interannual variability of pCO_2 increases further south into the SIZ than at the boundaries of the SIZ and open ocean. This is apparent even when possible, sampling biases due to sampling in different seasons are considered. To alleviate sampling/data biases, observational platforms such as biogeochemical Argo floats are already underway via the SOCCOM program (Sarmiento et al 2023) in the SIZ to overcome data sparsity and determine drivers that may be affecting the interannual variability of pCO_2 both on the large SO-scale and regional scale. This would also provide an opportunity to study the interannual variability of pCO_2 at different regions within the three basins. In addition, different response times result in the lag response of pCO_2 to the drivers - for instance, the collocated sea-ice concentration used in this study only focused on the specific years being investigated, and the previous years were not considered. A more informative approach to overcome the lag response could be to explore the ice concentration in the previous years (years before the actual years being investigated in the study) or investigate the interannual

variability of stratification. Moreover, a detailed study on the seasonal sea-ice properties, such as the rate of ice melt and formation and chlorophyll concentration, could be conducted to determine the magnitude of the sea-ice concentration's role in the interannual variability of pCO_2.

References

1. Abernathey, R. P., Cerovecki, I., Holland, P. R., Newsom, E., Mazloff, M., & Talley, L. D. (2016). Water-mass transformation by sea ice in the upper branch of the Southern Ocean overturning. *Nature Geoscience*, *9*(8), 596–601. https://doi.org/10.1038/ngeo2749
2. Angeles Gallego, M., Timmermann, A., Friedrich, T., & Zeebe, R. E. (2018). Drivers of future seasonal cycle changes in oceanic pCO2. *Biogeosciences*, *15*(17), 5315–5327. https://doi.org/10.5194/bg-15-5315-2018
3. Arroyo, M. C., Shadwick, E. H., & Tilbrook, B. (2019). Summer Carbonate Chemistry in the Dalton Polynya, East Antarctica. *Journal of Geophysical Research: Oceans*, *124*(8), 5634–5653. https://doi.org/10.1029/2018JC014882
4. Ayers, J. M., & Strutton, P. G. (2013). Nutrient variability in Subantarctic Mode Waters forced by the Southern Annular Mode and ENSO. *Geophysical Research Letters*, *40*(13), 3419–3423. https://doi.org/10.1002/grl.50638
5. Bakker, D. C. E., Hoppema, M., Wegener, A., Schröder, M., Geibert, W., Bakker, D. C. E., Hoppema, M., Schröder, M., Geibert, W., & De Baar, H. J. W. (2008). A rapid transition from ice-covered CO2-rich waters to a biologically mediated CO_2 sink in the eastern Weddell Gyre WedUP: Weddell Gyre Upwelling and Dynamical Processes View project PHYTOOPTICS-Helmholtz Young Investigator Group View project A rapid transition from ice-covered CO_2-rich waters to a biologically mediated CO_2 sink in the eastern Weddell Gyre. *Biogeosciences*, *5*, 1373–1386. https://doi.org/10.5194/bgd-5-1205-2008
6. Bakker, D. C. E., Pfeil, B., Landa, C. S., Metzl, N., O'Brien, K. M., Olsen, A., Smith, K., Cosca, C., Harasawa, S., Jones, S. D., Nakaoka, S. I., Nojiri, Y., Schuster, U., Steinhoff, T., Sweeney, C., Takahashi, T., Tilbrook, B., Wada, C., Wanninkhof, R., … Xu, S. (2016). A multi-decade record of high-quality fCO_2 data in version 3 of the Surface Ocean CO_2 Atlas (SOCAT). In *Earth System Science Data* (Vol. 8, Issue 2, pp. 383–413). Copernicus GmbH. https://doi.org/10.5194/essd-8-383-2016

7. Bakker, P., Schmittner, A., Lenaerts, J. T. M., Abe-Ouchi, A., Bi, D., van den Broeke, M. R., Chan, W. L., Hu, A., Beadling, R. L., Marsland, S. J., Mernild, S. H., Saenko, O. A., Swingedouw, D., Sullivan, A., & Yin, J. (2016). Fate of the Atlantic Meridional Overturning Circulation: Strong decline under continued warming and Greenland melting. *Geophysical Research Letters*, *43*(23), 12,252-12,260. https://doi.org/10.1002/2016GL070457
8. Barnes, E. A., & Hartmann, D. L. (2010). Dynamical feedback of the southern annular mode in winter and summer. *Journal of the Atmospheric Sciences*, *67*(7), 2320–2330. https://doi.org/10.1175/2010JAS3385.1
9. Boutin, J., Merlivat, L., Hénocq, C., Martin, N., & Sallée, J. B. (n.d.). *Air-sea CO_2 flux variability in frontal regions of the Southern Ocean from Carbon Interface Ocean Atmosphere drifters*. www.aslo.org/lo/toc/vol_53/issue_5_part_2/
10. Brown, P. J., Jullion, L., Landschützer, P., Bakker, D. C. E., Naveira Garabato, A. C., Meredith, M. P., Torres-Valdés, S., Watson, A. J., Hoppema, M., Loose, B., Jones, E. M., Telszewski, M., Jones, S. D., & Wanninkhof, R. (2015). Carbon dynamics of the Weddell Gyre, Southern Ocean. *Global Biogeochemical Cycles*, *29*(3), 288–306. https://doi.org/10.1002/2014GB005006
11. Craig, P. M., Ferreira, D., & Methven, J. (2017). The contrast between Atlantic and Pacific surface water fluxes. *Tellus, Series A: Dynamic Meteorology and Oceanography*, *69*(1). https://doi.org/10.1080/16000870.2017.1330454
12. DeVries, T. , H. M. & P. F. (2017). *Recent increase in oceanic carbon uptake driven by weaker upper-ocean overturning.* . 215–218.
13. Djeutchouang, L. M., Chang, N., Gregor, L., Vichi, M., & Monteiro, P. M. S. (2022). The sensitivity of pCO_2 reconstructions to sampling scales across a Southern Ocean sub-domain: a semi-idealized ocean sampling simulation approach. *Biogeosciences*, *19*(17), 4171–4195. https://doi.org/10.5194/bg-19-4171-2022
14. Doddridge, E. W., & Marshall, J. (2017). Modulation of the Seasonal Cycle of Antarctic Sea Ice Extent Related to the Southern Annular Mode. *Geophysical Research Letters*, *44*(19), 9761–9768. https://doi.org/10.1002/2017GL074319
15. Eayrs, C., Holland, D., Francis, D., Wagner, T., Kumar, R., & Li, X. (2019). Understanding the Seasonal Cycle of Antarctic Sea Ice Extent in the Context of Longer-Term

Variability. In *Reviews of Geophysics* (Vol. 57, Issue 3, pp. 1037–1064). Blackwell Publishing Ltd. https://doi.org/10.1029/2018RG000631

16. Elio Campitelli, L. B. D. & C. V. (2022). Assessment of zonally symmetric and asymmetric components of the Southern Annular Mode using a novel approach. *Climate Dynamics*, 161–178.
17. Fassbender, A. J., Rodgers, K. B., Palevsky, H. I., & Sabine, C. L. (2018). Seasonal Asymmetry in the Evolution of Surface Ocean pCO_2 and pH Thermodynamic Drivers and the Influence on Sea-Air CO_2 Flux. *Global Biogeochemical Cycles*, *32*(10), 1476–1497. https://doi.org/10.1029/2017GB005855
18. Fay, A. R., Gregor, L., Landschützer, P., McKinley, G. A., Gruber, N., Gehlen, M., Iida, Y., Laruelle, G. G., Rödenbeck, C., Roobaert, A., & Zeng, J. (2021). SeaFlux: Harmonization of air-sea CO_2 fluxes from surface pCO_2 data products using a standardized approach. In *Earth System Science Data* (Vol. 13, Issue 10, pp. 4693–4710). Copernicus Publications. https://doi.org/10.5194/essd-13-4693-2021
19. Fay, A. R., & McKinley, G. A. (2013). Global trends in surface ocean pCO2 from in situ data. *Global Biogeochemical Cycles*, *27*(2), 541–557. https://doi.org/10.1002/gbc.20051
20. Fay, A. R., & McKinley, G. A. (2017). Correlations of surface ocean pCO_2 to satellite chlorophyll on monthly to interannual timescales. *Global Biogeochemical Cycles*, *31*(3), 436–455. https://doi.org/10.1002/2016GB005563
21. Fogt, R. L., Jones, J. M., & Renwick, J. (2012). Seasonal zonal asymmetries in the southern annular mode and their impact on regional temperature anomalies. *Journal of Climate*, *25*(18), 6253–6270. https://doi.org/10.1175/JCLI-D-11-00474.1
22. Fogt, R. L., & Marshall, G. J. (2020). The Southern Annular Mode: Variability, trends, and climate impacts across the Southern Hemisphere. In *Wiley Interdisciplinary Reviews: Climate Change* (Vol. 11, Issue 4). Wiley-Blackwell. https://doi.org/10.1002/wcc.652
23. Fransson, A., Chierici, M., Miller, L. A., Carnat, G., Shadwick, E., Thomas, H., Pineault, S., & Papakyriakou, T. N. (2013). Impact of sea-ice processes on the carbonate system and ocean acidification at the ice-water interface of the Amundsen Gulf, Arctic Ocean.

Journal of Geophysical Research: Oceans, *118*(12), 7001–7023. https://doi.org/10.1002/2013JC009164

24. Fransson, A., Chierici, M., Yager, P. L., & Smith, W. O. (2011). Antarctic sea ice carbon dioxide system and controls. *Journal of Geophysical Research: Oceans*, *116*(12). https://doi.org/10.1029/2010JC006844
25. Friedlingstein, P., O'Sullivan, M., Jones, M. W., Andrew, R. M., Gregor, L., Hauck, J., Le Quéré, C., Luijkx, I. T., Olsen, A., Peters, G. P., Peters, W., Pongratz, J., Schwingshackl, C., Sitch, S., Canadell, J. G., Ciais, P., Jackson, R. B., Alin, S. R., Alkama, R., … Zheng, B. (2022). Global Carbon Budget 2022. *Earth System Science Data*, *14*(11), 4811–4900. https://doi.org/10.5194/essd-14-4811-2022
26. Frölicher, T. L., & Paynter, D. J. (2015). Extending the relationship between global warming and cumulative carbon emissions to multi-millennial timescales. *Environmental Research Letters*, *10*(7). https://doi.org/10.1088/1748-9326/10/7/075002
27. Geilfus, N. X., Carnat, G., Dieckmann, G. S., Halden, N., Nehrke, G., Papakyriakou, T., Tison, J. L., & Delille, B. (2013). First estimates of the contribution of $CaCO_3$ precipitation to the release of CO_2 to the atmosphere during young sea ice growth. *Journal of Geophysical Research: Oceans*, *118*(1), 244–255. https://doi.org/10.1029/2012JC007980
28. Geilfus, N. X., Galley, R. J., Else, B. G. T., Campbell, K., Papakyriakou, T., Crabeck, O., Lemes, M., Delille, B., & Rysgaard, S. (2016). Estimates of ikaite export from sea ice to the underlying seawater in a sea ice-seawater mesocosm. *Cryosphere*, *10*(5), 2173–2189. https://doi.org/10.5194/tc-10-2173-2016
29. Giddy, I. S., Nicholson, S. A., Queste, B. Y., Thomalla, S., & Swart, S. (2023). Sea-Ice Impacts Inter-Annual Variability of Phytoplankton Bloom Characteristics and Carbon Export in the Weddell Sea. *Geophysical Research Letters*, *50*(16). https://doi.org/10.1029/2023GL103695
30. Giddy, I., Swart, S., du Plessis, M., Thompson, A. F., & Nicholson, S. A. (2021). Stirring of Sea-Ice Meltwater Enhances Submesoscale Fronts in the Southern Ocean. *Journal of Geophysical Research: Oceans*, *126*(4). https://doi.org/10.1029/2020JC016814

31. Gregor, L., Kok, S., & Monteiro, P. M. S. (2017). Empirical methods for the estimation of Southern Ocean CO_2: Support vector and random forest regression. *Biogeosciences*, *14*(23), 5551–5569. https://doi.org/10.5194/bg-14-5551-2017
32. Gregor, L., Kok, S., & Monteiro, P. M. S. (2018). Interannual drivers of the seasonal cycle of CO_2 in the Southern Ocean. *Biogeosciences*, *15*(8), 2361–2378. https://doi.org/10.5194/bg-15-2361-2018
33. Gregor, L., Lebehot, A. D., Kok, S., & Scheel Monteiro, P. M. (2019). A comparative assessment of the uncertainties of global surface ocean CO_2 estimates using a machine-learning ensemble (CSIR-ML6 version 2019)-Have we hit the wall? *Geoscientific Model Development*, *12*(12), 5113–5136. https://doi.org/10.5194/gmd-12-5113-2019
34. Grimm, R., Notz, D., Glud, R. N., Rysgaard, S., & Six, K. D. (2016). Assessment of the sea-ice carbon pump: Insights from a three-dimensional ocean-sea-ice-biogeochemical model (MPIOM/HAMOCC). *Elementa: Science of the Anthropocene*, *4*. https://doi.org/10.12952/journal.elementa.000136
35. Gruber, N., Gloor, M., Mikaloff Fletcher, S. E., Doney, S. C., Dutkiewicz, S., Follows, M. J., Gerber, M., Jacobson, A. R., Joos, F., Lindsay, K., Menemenlis, D., Mouchet, A., Müller, S. A., Sarmiento, J. L., & Takahashi, T. (2009). Oceanic sources, sinks, and transport of atmospheric CO_2. *Global Biogeochemical Cycles*, *23*(1). https://doi.org/10.1029/2008GB003349
36. Gruber, N., Landschützer, P., Landschützer, L., & Lovenduski, N. S. (2018). *The Variable Southern Ocean Carbon Sink*. https://doi.org/10.1146/annurev-marine-121916
37. Hague, M., & Vichi, M. (n.d.). *Southern Ocean BGC-Argo Detect Under Ice Phytoplankton Growth Before Sea Ice Retreat*. https://doi.org/10.5194/bg-2020-257
38. Hauck, J., Völker, C., Wang, T., Hoppema, M., Losch, M., & Wolf-Gladrow, D. A. (2013). Seasonally different carbon flux changes in the Southern Ocean in response to the southern annular mode. *Global Biogeochemical Cycles*, *27*(4), 1236–1245. https://doi.org/10.1002/2013GB004600
39. Hewitt, H., Fox-Kemper, B., Pearson, B., Roberts, M., & Klocke, D. (2022). The small scales of the ocean may hold the key to surprises. *Nature Climate Change*, *12*(6), 496–499. https://doi.org/10.1038/s41558-022-01386-6

40. Holland, M. M., Landrum, L., Raphael, M., & Stammerjohn, S. (2017). Springtime winds drive the Ross Sea ice variability and change in the following autumn. *Nature Communications*, *8*(1). https://doi.org/10.1038/s41467-017-00820-0
41. Jersild, A., & Ito, T. (2020). Physical and Biological Controls of the Drake Passage pCO2 Variability. *Global Biogeochemical Cycles*, *34*(9). https://doi.org/10.1029/2020GB006644
42. Keppler, L., & Landschützer, P. (2019). Regional Wind Variability Modulates the Southern Ocean Carbon Sink. *Scientific Reports*, *9*(1). https://doi.org/10.1038/s41598-019-43826-y
43. Khatiwala, S., Tanhua, T., Mikaloff Fletcher, S., Gerber, M., Doney, S. C., Graven, H. D., Gruber, N., McKinley, G. A., Murata, A., Ríos, A. F., & Sabine, C. L. (2013). Global ocean storage of anthropogenic carbon. *Biogeosciences*, *10*(4), 2169–2191. https://doi.org/10.5194/bg-10-2169-2013
44. Kimura, N., Onomura, T., & Kikuchi, T. (2023). Processes governing seasonal and interannual change of the Antarctic sea-ice area. *Journal of Oceanography*, *79*(2), 109–121. https://doi.org/10.1007/s10872-022-00669-y
45. Kyle C Armour and Cecilia M Bitz. (2015). Observed and projected trends in Antarctic Sea Ice. *US CLIVAR VARIATIONS*, *13*(4).
46. Landschützer, P., Gruber, N., & Bakker, D. C. E. (2016). Decadal variations and trends of the global ocean carbon sink. *Global Biogeochemical Cycles*, *30*(10), 1396–1417. https://doi.org/10.1002/2015GB005359
47. Landschützer, P., Gruber, N., Bakker, D. C. E., & Schuster, U. (2014). Recent variability of the global ocean carbon sink. *Global Biogeochemical Cycles*, *28*(9), 927–949. https://doi.org/10.1002/2014GB004853
48. Landschützer, P., Gruber, N., Bakker, D. C. E., Stemmler, I., & Six, K. D. (2018). Strengthening seasonal marine CO_2 variations due to increasing atmospheric CO2. *Nature Climate Change*, *8*(2), 146–150. https://doi.org/10.1038/s41558-017-0057-x
49. Landschützer, P., Gruber, N., Haumann, F. A., Rödenbeck, C., Bakker, D. C. E., Van Heuven, S., Hoppema, M., Metzl, N., Sweeney, C., Takahashi, T., Tilbrook, B., & Wanninkhof, R. (2015). The reinvigoration of the Southern Ocean carbon sink. *Science*, *349*(6253), 1221–1224. https://doi.org/10.1126/science.aab2620

50. Large, W. G. and P. S. (1981). Open Ocean Momentum Flux Measurements in Moderate to Strong Winds. *Journal of Physical Oceanography*, *11*, 324–336.
51. Le Quéré, C., Raupach, M. R., Canadell, J. G., Marland, G., Bopp, L., Ciais, P., Conway, T. J., Doney, S. C., Feely, R. A., Foster, P., Friedlingstein, P., Gurney, K., Houghton, R. A., House, J. I., Huntingford, C., Levy, P. E., Lomas, M. R., Majkut, J., Metzl, N., … Woodward, F. I. (2009). Trends in the sources and sinks of carbon dioxide. *Nature Geoscience*, *2*(12), 831–836. https://doi.org/10.1038/ngeo689
52. Lee, D. Y., Petersen, M. R., & Lin, W. (2019). The Southern Annular Mode and Southern Ocean Surface Westerly Winds in E3SM. *Earth and Space Science*, *6*(12), 2624–2643. https://doi.org/10.1029/2019EA000663
53. Lefebvre, W., Goosse, H., Timmermann, R., & Fichefet, T. (2004). Influence of the Southern Annular Mode on the sea ice - Ocean system. *Journal of Geophysical Research: Oceans*, *109*(9), 1–12. https://doi.org/10.1029/2004JC002403
54. Legge, O. J., Bakker, D. C. E., Meredith, M. P., Venables, H. J., Brown, P. J., Jones, E. M., & Johnson, M. T. (2017). The seasonal cycle of carbonate system processes in Ryder Bay, West Antarctic Peninsula. *Deep-Sea Research Part II: Topical Studies in Oceanography*, *139*, 167–180. https://doi.org/10.1016/j.dsr2.2016.11.006
55. Lenton, A., & Matear, R. J. (2007). Role of the Southern Annular Mode (SAM) in Southern Ocean CO_2 uptake. *Global Biogeochemical Cycles*, *21*(2). https://doi.org/10.1029/2006GB002714
56. Lenton, A., Tilbrook, B., Law, R. M., Bakker, D., Doney, S. C., Gruber, N., Ishii, M., Hoppema, M., Lovenduski, N. S., Matear, R. J., McNeil, B. I., Metzl, N., Fletcher, S. E. M., Monteiro, P. M. S., Rödenbeck, C., Sweeney, C., & Takahashi, T. (2013). Sea-air CO_2 fluxes in the Southern Ocean for the period 1990-2009. *Biogeosciences*, *10*(6), 4037–4054. https://doi.org/10.5194/bg-10-4037-2013
57. Lovenduski, N. S., & Gruber, N. (2005). Impact of the Southern Annular Mode on Southern Ocean circulation and biology. *Geophysical Research Letters*, *32*(11), 1–4. https://doi.org/10.1029/2005GL022727
58. Lovenduski, N. S., Gruber, N., Doney, S. C., & Lima, I. D. (2007). Enhanced CO_2 outgassing in the Southern Ocean from a positive phase of the Southern Annular Mode. *Global Biogeochemical Cycles*, *21*(2). https://doi.org/10.1029/2006GB002900

59. Majkut, J. D., Sarmiento, J. L., & Rodgers, K. B. (2014). A growing oceanic carbon uptake: Results from an inversion study of surface pCO_2 data. *Global Biogeochemical Cycles*, *28*(4), 335–351. https://doi.org/10.1002/2013GB004585
60. Marshall, J., & Speer, K. (2012). Closure of the meridional overturning circulation through Southern Ocean upwelling. In *Nature Geoscience* (Vol. 5, Issue 3, pp. 171–180). https://doi.org/10.1038/ngeo1391
61. Matear, R. J., Hirst, A. C., & McNeil, B. I. (2000). Changes in dissolved oxygen in the Southern Ocean with climate change. *Geochemistry, Geophysics, Geosystems*, *1*(11). https://doi.org/10.1029/2000GC000086
62. Metzl, N., Brunet, C., Jabaud-Jan, A., Poisson, A., & Schauer, B. (2006). Summer and winter air–sea CO_2 fluxes in the Southern Ocean. *Deep Sea Research Part I: Oceanographic Research Papers*, *53*(9), 1548–1563. https://doi.org/https://doi.org/10.1016/j.dsr.2006.07.006
63. Mikaloff Fletcher, S. E., Gruber, N., Jacobson, A. R., Doney, S. C., Dutkiewicz, S., Gerber, M., Follows, M., Joos, F., Lindsay, K., Menemenlis, D., Mouchet, A., Müller, S. A., & Sarmiento, J. L. (2006). Inverse estimates of anthropogenic CO2 uptake, transport, and storage by the ocean. *Global Biogeochemical Cycles*, *20*(2). https://doi.org/10.1029/2005GB002530
64. Miller, K. G., Mountain, G. S., Wright, J. D., & Browning, J. V. (2011). Sea level and ice volume variations from continental margin and deep-sea isotopic records. *Oceanography*, *24*(2), 40–53. https://doi.org/10.5670/oceanog.2011.26
65. Monteiro, P. M. S., Dewitte, B., Scranton, M. I., Paulmier, A., & Van Der Plas, A. K. (2011). The role of open ocean boundary forcing on seasonal to decadal-scale variability and long-term change of natural shelf hypoxia. *Environmental Research Letters*, *6*(2). https://doi.org/10.1088/1748-9326/6/2/025002
66. Monteiro, P. M. S., Gregor, L., Lévy, M., Maenner, S., Sabine, C. L., & Swart, S. (2015). Intraseasonal variability linked to sampling alias in air-sea CO2 fluxes in the Southern Ocean. *Geophysical Research Letters*, *42*(20), 8507–8514. https://doi.org/10.1002/2015GL066009
67. Moreau, S., Vancoppenolle, M., Bopp, L., Aumont, O., Madec, G., Delille, B., Tison, J. L., Barriat, P. Y., & Goosse, H. (2016). Assessment of the sea-ice carbon pump: Insights

from a three-dimensional ocean-sea-ice biogeochemical model (NEMO-LIM-PISCES). *Elementa*, *2016*. https://doi.org/10.12952/journal.elementa.000122

68. Munro, D. R., Lovenduski, N. S., Takahashi, T., Stephens, B. B., Newberger, T., & Sweeney, C. (2015). Recent evidence for a strengthening CO_2 sinks in the Southern Ocean from carbonate system measurements in the Drake Passage (2002-2015). *Geophysical Research Letters*, *42*(18), 7623–7630. https://doi.org/10.1002/2015GL065194
69. Nicholson, S. A., Whitt, D. B., Fer, I., du Plessis, M. D., Lebéhot, A. D., Swart, S., Sutton, A. J., & Monteiro, P. M. S. (2022). Storms drive outgassing of CO_2 in the subpolar Southern Ocean. *Nature Communications*, *13*(1). https://doi.org/10.1038/s41467-021-27780-w
70. Nomura, D., Yoshikawa-Inoue, H., & Toyota, T. (2006). The effect of sea-ice growth on air-sea CO_2 flux in a tank experiment. *Tellus, Series B: Chemical and Physical Meteorology*, *58*(5), 418–426. https://doi.org/10.1111/j.1600-0889.2006.00204.x
71. Ogundare, M. O., Fransson, A., Chierici, M., Joubert, W. R., & Roychoudhury, A. N. (2021). Variability of Sea-Air Carbon Dioxide Flux in Autumn Across the Weddell Gyre and Offshore Dronning Maud Land in the Southern Ocean. *Frontiers in Marine Science*, *7*. https://doi.org/10.3389/fmars.2020.614263
72. Parkinson, C. L. (2019). A 40-year record reveals gradual Antarctic Sea Ice increases followed by decreases at rates far exceeding the rates seen in the Arctic. *Proceedings of the National Academy of Sciences of the United States of America*, *116*(29), 14414–14423. https://doi.org/10.1073/pnas.1906556116
73. Pasquer, B., Metzl, N., Goosse, H., & Lancelot, C. (2015). What drives the seasonality of air-sea CO_2 fluxes in the ice-free zone of the Southern Ocean: A 1D coupled physical-biogeochemical model approach. *Marine Chemistry*, *177*, 554–565. https://doi.org/10.1016/j.marchem.2015.08.008
74. Pitcher, G. C., Figueiras, F. G., Hickey, B. M., & Moita, M. T. (2010). The physical oceanography of upwelling systems and the development of harmful algal blooms. *Progress in Oceanography*, *85*(1–2), 5–32. https://doi.org/10.1016/j.pocean.2010.02.002

75. Precious Mongwe, N., Vichi, M., & Monteiro, P. M. S. (2018). The seasonal cycle of pCO_2 and CO_2 fluxes in the Southern Ocean: Diagnosing anomalies in CMIP5 Earth system models. *Biogeosciences*, *15*(9), 2851–2872. https://doi.org/10.5194/bg-15-2851-2018
76. Prend, C. J., Gray, A. R., Talley, L. D., Gille, S. T., Haumann, F. A., Johnson, K. S., Riser, S. C., Rosso, I., Sauvé, J., & Sarmiento, J. L. (2022). Indo-Pacific Sector Dominates Southern Ocean Carbon Outgassing. *Global Biogeochemical Cycles*, *36*(7). https://doi.org/10.1029/2021GB007226
77. Resplandy, L., Boutin, J., & Merlivat, L. (2014). Observed small spatial scale and seasonal variability of the CO_2 system in the Southern Ocean. *Biogeosciences*, *11*(1), 75–90. https://doi.org/10.5194/bg-11-75-2014
78. Rintoul, S. R. (2018). The global influence of localized dynamics in the Southern Ocean. *Nature*, *558*(7709), 209–218. https://doi.org/10.1038/s41586-018-0182-3
79. Ritter, R., Landschützer, P., Gruber, N., Fay, A. R., Iida, Y., Jones, S., Nakaoka, S., Park, G. H., Peylin, P., Rödenbeck, C., Rodgers, K. B., Shutler, J. D., & Zeng, J. (2017). Observation-Based Trends of the Southern Ocean Carbon Sink. *Geophysical Research Letters*, *44*(24), 12,339-12,348. https://doi.org/10.1002/2017GL074837
80. Rysgaard, S., Glud, R. N., Sejr, M. K., Bendtsen, J., & Christensen, P. B. (2007). Inorganic carbon transport during sea ice growth and decay: A carbon pump in polar seas. *Journal of Geophysical Research: Oceans*, *112*(3). https://doi.org/10.1029/2006JC003572
81. Sabine, C. L., Feely, R. A., Gruber, N., Key, R. M., Lee, K., Bullister, J. L., Wanninkhof, R., Wong, C. S., Wallace, D. W. R., Tilbrook, B., Millero, F. J., Peng, T.-H., Kozyr, A., Ono, T., & Rios, A. F. (n.d.). *The Oceanic Sink for Anthropogenic CO_2*. http://science.sciencemag.org/
82. Sallée, J. B., Speer, K. G., & Rintoul, S. R. (2010). Zonally asymmetric response of the Southern Ocean mixed-layer depth to the Southern Annular Mode. *Nature Geoscience*, *3*(4), 273–279. https://doi.org/10.1038/ngeo812
83. Sarmiento, J. L., Gruber, N., Brzezinski, M. A., & Dunne, J. P. (2004). High-latitude controls of thermocline nutrients and low-latitude biological productivity. *Nature*, *427*(6969). https://doi.org/10.1038/nature02127

84. Schossler, V., Aquino, F. E., Reis, P. A., & Simões, J. C. (2020). Antarctic atmospheric circulation anomalies and explosive cyclogenesis in the spring of 2016. *Theoretical and Applied Climatology*, *141*(1–2), 537–549. https://doi.org/10.1007/s00704-020-03200-9

85. Shadwick, E. H., De Meo, O. A., Schroeter, S., Arroyo, M. C., Martinson, D. G., & Ducklow, H. (2021). Sea Ice Suppression of CO2 Outgassing in the West Antarctic Peninsula: Implications For The Evolving Southern Ocean Carbon Sink. *Geophysical Research Letters*, *48*(11). https://doi.org/10.1029/2020GL091835

86. Shetye, S. S., Mohan, R., Patil, S., Jena, B., Chacko, R., George, J. V., Noronha, S., Singh, N., Priya, L., & Sudhakar, M. (2015). Oceanic pCO_2 in the Indian sector of the Southern Ocean during the austral summer–winter transition phase. *Deep Sea Research Part II: Topical Studies in Oceanography*, *118*. https://doi.org/10.1016/j.dsr2.2015.05.017

87. Simpkins, G. R., Ciasto, L. M., Thompson, D. W. J., & England, M. H. (2012). Seasonal relationships between large-scale climate variability and antarctic sea ice concentration. *Journal of Climate*, *25*(16), 5451–5469. https://doi.org/10.1175/JCLI-D-11-00367.1

88. Sloyan, B. M., & Rintoul, S. R. (2001). The Southern Ocean limb of the global deep overtuning circulation. *Journal of Physical Oceanography*, *31*(1), 143–173. https://doi.org/10.1175/1520-0485(2001)031<0143:TSOLOT>2.0.CO;2

89. Speich, S., Blanke, B., & Cai, W. (2007). Atlantic meridional overturning circulation and the Southern Hemisphere supergyre. *Geophysical Research Letters*, *34*(23). https://doi.org/10.1029/2007GL031583

90. Swart, S., Du Plessis, M. D., Nicholson, S. A., Monteiro, P. M. S., Dove, L. A., Thomalla, S., Thompson, A. F., Biddle, L. C., Edholm, J. M., Giddy, I., Heywood, K. J., Lee, C., Mahadevan, A., Shilling, G., & De Souza, R. B. (2023). The Southern Ocean mixed layer and its boundary fluxes: Fine-scale observational progress and future research priorities. In *Philosophical Transactions of the Royal Society A: Mathematical, Physical and Engineering Sciences* (Vol. 381, Issue 2249). Royal Society Publishing. https://doi.org/10.1098/rsta.2022.0058

91. Takahashi, T., Sutherland, S. C., Sweeney, C., Poisson, A., Metzl, N., Tilbrook, B., Bates, N., Wanninkhof, R., Feely, R. A., Sabine, C., Olafsson, J., & Nojiri, Y. (2002). Global sea-

air CO_2 flux based on climatological surface ocean pCO_2 , and seasonal biological and temperature effects. In */ Deep-Sea Research II* (Vol. 49).

92. Thomalla, S. J., Fauchereau, N., Swart, S., & Monteiro, P. M. S. (2011). Regional scale characteristics of the seasonal cycle of chlorophyll in the Southern Ocean. *Biogeosciences*, *8*(10), 2849–2866. https://doi.org/10.5194/bg-8-2849-2011
93. Thompson, D. W. J., & Solomon, S. (2002). Interpretation of recent Southern Hemisphere climate change. *Science*, *296*(5569), 895–899. https://doi.org/10.1126/science.1069270
94. Turner, J., Holmes, C., Caton Harrison, T., Phillips, T., Jena, B., Reeves-Francois, T., Fogt, R., Thomas, E. R., & Bajish, C. C. (2022). Record Low Antarctic Sea Ice Cover in February 2022. *Geophysical Research Letters*, *49*(12). https://doi.org/10.1029/2022GL098904
95. Visbeck, M., & Hall, A. (2004). *2255 Reply **.
96. Wanninkhof, R., Asher, W. E., Ho, D. T., Sweeney, C., & McGillis, W. R. (2009). Advances in quantifying air-sea gas exchange and environmental forcing. In *Annual Review of Marine Science* (Vol. 1, pp. 213–244). https://doi.org/10.1146/annurev.marine.010908.163742
97. Williams, N. L., Juranek, L. W., Feely, R. A., Russell, J. L., Johnson, K. S., & Hales, B. (2018). Assessment of the Carbonate Chemistry Seasonal Cycles in the Southern Ocean from Persistent Observational Platforms. *Journal of Geophysical Research: Oceans*, *123*(7), 4833–4852. https://doi.org/10.1029/2017JC012917